Review Article

Adsorption of Heavy Metals in Contaminated Water Using Zeolite Derived from Agro-Wastes and Clays: A Review

Ismael Kithinji Kinoti [ID],[1] Joanne Ogunah,[2] Cyprian Muturia M'Thiruaine,[1] and Joseph Mwiti Marangu [ID][1]

[1]*Physical Sciences, Meru University of Science and Technology, Meru, Kenya*
[2]*Department of Physical Sciences, University of Embu, Embu, Kenya*

Correspondence should be addressed to Joseph Mwiti Marangu; jmarangu2011@gmail.com

Due to climate change and anthropogenic activities such as agriculture, mining, and urbanization, water contamination has become a very real modern problem. Modern solutions such as activated carbon, reverse osmosis, and ultrafiltration, among others, have been employed in the decontamination of water. These methods are, however, expensive to set up and maintain and therefore have proved a challenge to implement in developing countries. Zeolite materials exhibit excellent structural properties, such as high ion exchange capacity, porosity, and relative surface area, which make them attractive to water decontamination processes. However, conventional zeolites are expensive, and recent research has focused on utilizing low-cost materials such as agro-wastes and clays as raw materials for the synthesis of zeolites. This review aims to discuss the role of low-cost zeolites in their removal of heavy metals and the feasibility of agro-wastes and natural clays in the synthesis of zeolites. Recent research studies based on the synthesis of zeolites from clays and agro-wastes and their application in heavy metal removal have been reviewed and discussed. Agro-wastes such as rice husk ash and sugarcane bagasse ash and layered silicate clays such as kaolinite and smectites are particularly of interest to zeolite synthesis due to their high silica to alumina ratio. Zeolites synthesized through various methods such as hydrothermal, molten salt, and microwave irradiation synthesis have been discussed with their effect on the adsorption of various heavy metals.

1. Introduction

Water utilization for domestic, industrial, or agricultural purposes gives rise to different forms of wastewater [1] in a continuous process due to the never-ending stream of human activities requiring usage of water. According to UN-WWDR [2], over 80% of global wastewater is released to the environment without undergoing proper treatment. This brings about 1.8 billion people at risk of waterborne diseases, owing to contaminated water sources [3]. Dye contaminants resulting from artificial pigments are some of the largest water contaminants in the world. It is estimated that the dye industry discharges approximately 7.5 metric tons to the environment every year [4]. Contaminants such as methylene and celestine blue [5], rhodamine, and crystal violet

[6], among others, are known to cause poor light penetration to water bodies, thereby hindering photosynthesis and consequently death to aquatic life. In response to a growing population and economy in most low and lower-middle income countries, exposure to contaminants is only estimated to increase, according to a report by UNEP [7]. With the most agricultural system incorporating modern techniques of farming and especially use of herbicides, they are also becoming a common contaminant in most water systems. Fenuron for instance, a common herbicide used to control growth of weeds, is suspected to be carcinogenic to human beings [8] and highly toxic if ingested in large amounts [9]. It is estimated that only 1% of pesticides and herbicides reach their intended target and the rest finds its way to soil, water systems, and vegetables and other

consumable crops [9]. Heavy metals, on the other hand, are recognized as the most poisonous contaminants with adverse effects to the environment and health in general [10].

Wastewater has been classified as domestic, industrial, or storm wastewater [2]. Domestic wastewater arises from domestic water uses in homes or business premises such as cleaning, laundry, and toilet flushing, among others. Domestic wastewater mainly comprises detergent chemicals, fecal matter and urine, and bleach, among other substances [11]. Industrial wastewater arises from industrial processes such as cooling processes or as byproducts of industrial processes. Industrial wastewater can be highly toxic to the environment depending on the involved industrial process [12]. Storm wastewater is generally water due to natural processes such as rainfall and mainly comprises eroded material and other particular matter depending on where the water has runoff [13]. Urban storm water mainly contains heavy metals and other toxic materials due to runoff from open garages and carwashes, especially in many developing countries, where wastewater treatment plans are not available for such small businesses [14]. In cases where there are treatment systems in place inclusive of municipal wastewater treatment systems, major focus is on the removal of biological and solid pollutants through biological treatments in stabilization [15]. However, toxic elements of the wastewater such as heavy metals are left untreated despite the fact that they pose a major health concern [16]. Many methods have been adopted for the removal of heavy metals from wastewater. Use of nanocomposites of multiwalled carbon nanotubes [17, 18], magnetic composites of Fe_3O_4 [19], and activated carbon [20], among others, have been employed on the small scale. Modern large-scale implementations of water purification systems capable of removing heavy metals is often through reverse osmosis, ultrafiltration, and ion exchange, among others, that are unfortunately not accessible to most low and middle-income countries due to high costs of operation and maintenance [21].

Heavy metals are elements considered to have a relatively high atomic weight or density [22]. These include cadmium, copper, iron, chromium, and lead, among others. Some of these metals in trace amounts are useful in the human body, often taking part in crucial processes such as iron in the formation of hemoglobin [23], copper in the efficient absorption of iron into the body [24], and zinc in the synthesis of proteins in the body [25]. Other heavy metals tend to bioaccumulate in the bloodstream and thus become toxic, often causing adverse effects on the human body. Cadmium, for example, on finding its way to the human body and ultimately to the liver, will cause hepatotoxicity and bioaccumulation in the kidneys in the renal tissues causing nephrotoxicity [26]. In chromium, the oxidized states of Cr (VI) are considered very toxic because of the high solubility in water and mobility. Chromium permissible limits in water are set to 0.1 mg/L according to USEPA [27]. Arsenic is often found in dyes, paints, drugs, and semiconductors, among other sources. It can occur as either arsenite or arsenate in organic or inorganic forms, both of which are harmful to human beings. Chronic toxicity is characterized by keratosis and pigmentation issues [28]. Long-term exposure to arsenic compounds has been associated with neurological issues, diabetes mellitus, and cardiovascular diseases, among others [29]. Arsenic permissible limit is 0.01 mg/L according to WHO in water [30]. Lead contamination occurs from effluents of battery repair or production industries, cosmetic, ammunition, soldering, or old pipes. Children are said to bioabsorb 50% more lead than adults during their development [29]. Due to its ability to be biodeposited into the body, it is reported that 95% of lead once in human body can be deposited as a form of insoluble phosphate in skeletal bones. Acute poisoning of lead has been linked with headaches, loss of appetite, arthritis, and hallucination, among other effects. Chronic effects include mental retardation, psychosis, birth defects, autism, and kidney damage, among others [31]. Allowable limit of lead in drinking water according to WHO is 0.01 mg/L [32]. This article reviews the structure and properties of zeolites derived from agro-based materials and clays, their methods of synthesis, efficiencies for removal of heavy metals in wastewaters, and the challenges or recommendations around the utilization of the derived zeolites.

2. Wastewater Treatment Processes

Wastewater is made up of solids (350–1200 mg/l), dissolved and particulate matter (250–1000 mg/l), microorganisms (up to 109 numbers/ml) and nutrients, heavy metals, and micropollutants [33]. The most problematic pollutants are solids, as they can clog and/or damage the system. The role of wastewater treatment is to convert the influent into a state that can safely be returned back to the water cycle without negatively impacting the environment [1]. To achieve this, physical [9], chemical [34], and biological processes are applied through the stages of treatment discussed. These stages are summarized in Figure 1.

2.1. Preliminary Treatment. This stage involves the removal of grit and large solids that would damage equipment in later stages or be too large to continue the process [36]. At this stage, plastics, pieces or blocks of wood, metals and glass material, as well as surface oil, gravel, and sand due to stormwater are removed using mechanical and physical-chemical methods [35]. The principle of treatment at the preliminary step is based on the particle size of the contaminant; therefore, size exclusion techniques are indispensable. These include use of screens, comminutors, grit-removers, and skimming tanks [37]. Screening devices are made up of wire mesh, parallel bars, grating, perforated plates, etc., to make uniform size openings usable in the removal of floating matter, often referred to as rakings or screenings. It has been found that sanitary sewage (domestic sewage) makes use of an average of 0.0015–0.015 m^3/Ml screenings with an average screen size of 25–100 mm [37]. The screenings are disposed off through incineration, burial, digestion, or composting.
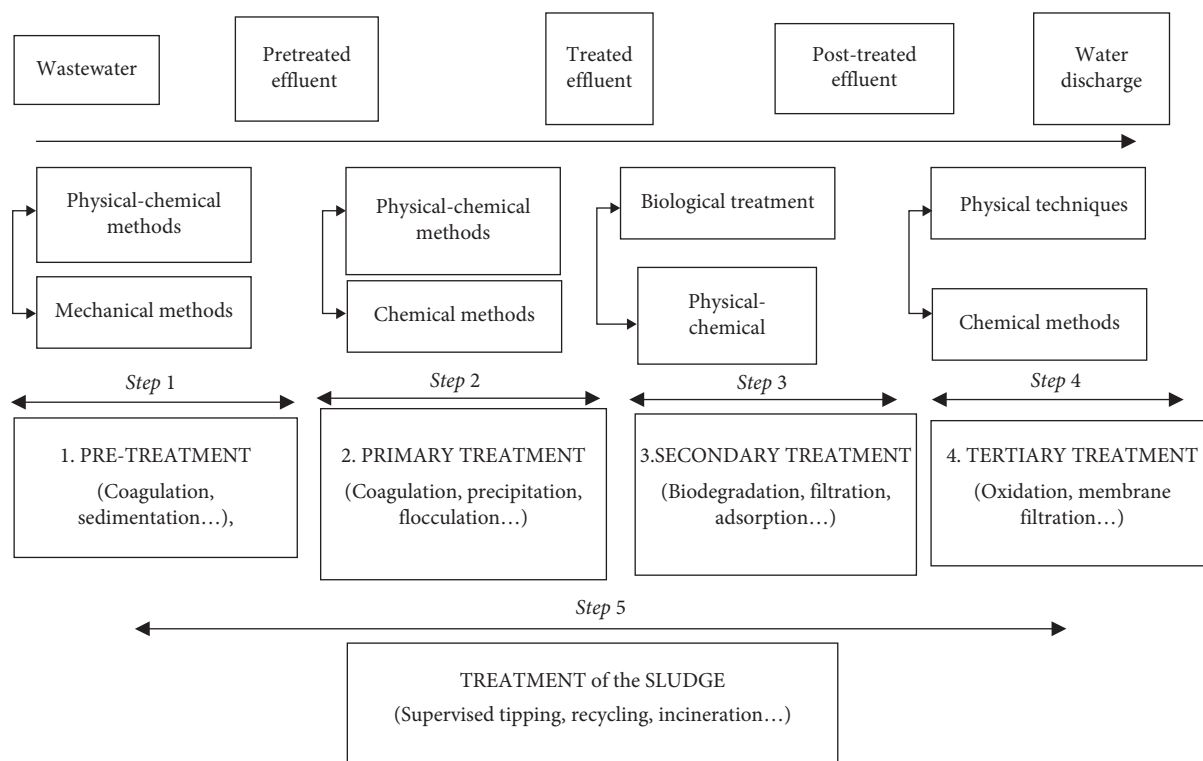
FIGURE 1: Summary of wastewater treatment processes (adopted from [35]).

2.2. Primary Step. The most prominent method of wastewater treatment at this stage is the physical process, which involves sedimentation by the use of membrane filters that require frequent backwash, which can incur extra costs [38]. However, chemical processes may be employed to induce coagulation and flocculation of suspended materials that will not settle through gravity [39]. By the use of sedimentation and floatation, both inorganic and organic solids are removed from wastewater at this stage. Common contaminants removed at this stage include biochemical oxygen demand, total suspended solids, grease and oils, organic nitrogen, organic phosphorus, and traces of heavy metals. The primary stage manages the removal of 50–70% of the suspended solids and 25–50% of the biochemical oxygen demand [40]. Treatment units that have been applied at this stage include detritus tanks, grit chambers, skimming tanks, screens, and primary sedimentation tanks [41]. The screens at this stage are used in the removal of floating matter with comparatively large particle size. Detritus tanks are used when the flow velocity is low, and they withhold sewage for longer periods (approximately 4 minutes), thereby removing fine settleable particles [41]. In the primary step, chemical precipitation is considered only in special cases where (i) odor becomes a problem; (ii) there is a need to remove phosphorus compounds; (iii) there is industrial waste that is likely to destabilize the biological removal process; and (iv) the strength and flow of the wastewater vary greatly [42].

2.3. Secondary Step. This stage incorporates the use of biological and chemical techniques in the treatment of wastewater from the primary step [43]. Microorganisms are used in the removal of most inorganic and organic contaminants, followed by chemical filtration to remove pathogens [38]. Trickling filters are used to induce the decomposition of organic pollutants in biofilms, a process aided by aerobic or anaerobic microorganisms [38]. About 85% of BOD and TSS are removable at this stage, leaving traces of heavy metals, phosphorus, nitrogen, pathogens, and bacteria for removal at the tertiary stage [44]. Conventional processes applied at this stage include trickling filters, oxidation ponds, activated sludge, and filter pods. Space, initial, and operational costs are factors that determine the choice of an applicable technique in secondary sewage treatment [43]. Often, space is a limiting factor due to the high municipal or local area population and the cost of the land. Therefore, this makes oxidation ponds uneconomical and least adopted in regions where land costs are high [43]. Activated sludge, on the other hand, is widely used since it requires low space, minimizes construction costs, and produces a relatively low odor. This method, however, can be costly to operate owing to energy expenses for the oxygen demand and the air pump operation costs [45]. The trickling filter method offers biological contaminant removal through the salts, rocks, plastics, or stones. These are usually packed in such a way that they allow growth of microorganisms and sewage flow through, in very low velocities, to

ensure ample contact with the microorganisms [46]. The filters have relatively low construction cost, provide a cheap system of oxygen delivery, and can exist with nonelectric systems. However, they are temperature-dependent, can be easily congested, and occupy a larger surface area compared to activated sludge types [43].

2.4. Tertiary Step. This stage involves the disinfection of the water to make it reusable again. In this step, chemical processes like chlorination for removal of residual pathogenic bacteria and more specific adsorbents for the removal of toxic elements like dyes and notorious heavy metals are incorporated [47]. The chlorination process, although often applied due to its effectiveness in disinfection, easy to use, and budget friendly, can be hazardous if used in excess [47]. Chlorinated water is freed from harmful microbes, but for disposal into aquatic ecosystems, it needs to be dechlorinated, as chlorine can form potentially carcinogenic compounds such as mutagen X [48] and trihalomethanes [49] when it reacts with some organic materials. Recently, ultraviolet (UV) light [38] and ozone [47] are being employed for disinfection without alteration of the water quality. In UV treatment, the water effluent is passed through ultraviolet radiation, which alters the genetic structure, thus rendering them sterile and unable to infect wildlife or humans. However, the water needs to have undergone thorough pretreatment before this step since residual organic matter can reduce the UV light effectiveness when they shield the microbes [47]. The downside of UV treatment is the relatively high costs of maintenance of the UV lamps. In ozone treatment, microbes are destroyed on contact with ozone and forms no hazardous byproducts [50]. The use of ozone is convenient since it can be produced as needed onsite and needs no storage; equipment, however, can be expensive to maintain [15]. The final stage in the tertiary step must be filtration, which can be achieved using activated carbon fibers, sand or disc, and drum or bag filters [47]. When it is necessary to reduce a contaminant to a specific micron concentration rating, bag filters are used [51]. Drum filters have woven cloth wrapped over a drum, through which the influent gets into the drum and filtrate out the cloth. Backwash removes contaminants and ensures the continuous functioning of the system [52].

Although these three waste water treatment steps are required for any waste water treatment plant, most of the plants in low- and middle-income countries have reported low efficiencies in the removal of heavy metals.

3. Wastewater Treatment Technologies

3.1. Ion Exchange. Ion exchange has seen great usage in the removal of heavy metals in the water purification process, whereby cations are used to exchange for metal ions in water through physical or chemical processes [53]. An electrostatic field often binds exchangeable ions onto functional groups available on a solid matrix that needs to come into contact with mobile contaminated water to remove the metal ions [54]. Varying experimental conditions affect the affinity of

the ion exchange for certain species, thereby separating them from the solution [54]. Ion exchangers often make use of natural zeolites and synthetic resins to remove metal ions [53]. The resins (R) work through hydrogen-based ion exchange where the cation exchanger releases its hydrogen ion (H^+) into the solution to exchange for an ion (X^+) in the solution as follows [54]:

$$R - H + X^+ \leftrightarrow R - X + H^+. \tag{1}$$
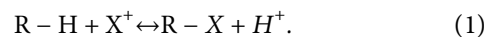
Every ion removed from the solution is replaced by another, thus achieving a state of electroneutrality. Several types of ion exchangers including zeolites structured into ion exchangers have been utilized in the removal of heavy metals. Luca [55] comparatively studied the removal of zinc by zeolite ETS-10-based ion exchanger against municipal zeolite A-based ion exchanger and reported higher removal by ETS-10. A different paper by Kumar [56] studied the adsorption of lead (II) ions on a hybrid ion exchanger and reported maximum adsorption capacity 182.7 mg/g ions at 50°C. The adsorption was reported to follow a pseudo-second-order kinetic model for the adsorbed ion. In a similar paper by Ma et al. [57], upon removal of nickel ions using dual-exchanged (Na^+/H^+) chelating resin, metal ion removal was reported to be highly dependent on the pH of the solution and the Na^+ to H^+ ratio. High concentrations of sodium ions led to precipitation of nickel hydroxide, which clogged the ion exchanger. Too much hydrogen ions led to competitive protonation, whose consequence was noted to be reduced nickel ion uptake. The heavy metal ion exchanger method is effective with high metal ion removal efficiency, high selectivity, and rapid adsorption kinetics and is applicable in the whole water treatment range [58]. These advantages have seen its massive utilization in most water purification systems especially in developed countries. The method, however, suffers major challenges such as high operating costs and production of sludge which is expensive to process; resins are easily polluted by organic contaminants, and in the face of heavy pollution, resins spend easily [59].

3.2. Reverse Osmosis. Reverse osmosis (RO) technology makes use of semipermeable membranes (filters) to remove contaminants from water by allowing only water to pass through [60]. With the membrane pore size in the range 0.1–1.0 nm, an applied pressure is necessary to overcome osmotic pressure, thereby requiring high energy to operate [61]. The performance of RO filters is greatly affected by the characteristics of the feed water, such as temperature, salt concentration of the feedwater, and the aforementioned pressure [62]. Generally, a higher feedwater temperature ensures high permeate flow due to increased diffusion rates and lower viscosity associated with higher temperatures. The pressure parameter referred to as net driving pressure (NDP), which is the cumulative sum of all the forces exerted on the RO membrane, is often used to understand the feed pressure [63]. Doubling the NDP hypothetically doubles the flow of the permeate [64]. As water flows through the RO membrane, the TDS concentration on the influent side will

always be higher than that on the effluent side and so will the pressure. A gradient of salt concentration parameter, determined as the difference between influent and effluent TDS of an RO, describes salt rate passage in an RO system. The passage is usually independent of the pressure in the system [62].

In recent years, different studies have been conducted to bring solutions for heavy metal removal using reverse osmosis technology. Thaci and Gashi [65] utilized biowaste materials to design water purification systems, utilizing the material as a guide with reverse osmosis technology to remove contaminants such as lead, zinc, cadmium, cobalt, manganese, and nickel. Others have used spiral bound reverse osmosis membrane [66] and antifouling reverse osmosis membrane using crosslinkers [67], among others.

Reverse osmosis method is very effective in water purification system as it only allows water to pass through by blocking all other ions. It requires simple maintenance, and it is preferred because it does not require chemicals to remove ion contaminants [68]. It is, however, prone to clogging, fouling, and scaling and therefore requires frequent filter change and maintenance [69]. This increases maintenance costs. In addition, reverse osmosis is slow in operation and often not self-sustainable [70].

3.3. Electrodialysis.

Electrodialysis is often used as a modification of ion exchange membranes to make them more selective in their contaminant removal or to improve their removal capabilities [61]. Ionic and cationic membranes with embedded electrodialysis stacks are sandwiched by two electrodes. With the application of an electric current, anions and cations pass through the electrodialysis membrane and are retained on the ion exchange membranes, thus creating a divided aqueous solution with concentrate (high content of contaminants) and diluent [71]. Since electrodialysis uses membranes, it is applicable in low TSS wastewater with suspended particle diameter not higher than $10\,\mu m$ [72]. The larger particle size clogs the membranes. Wastewater needs to contain TDS concentrations of not more than 5000 mg/l for effective removal [73]. Other important factors that affect the functioning of an electrodialysis system include the flow rate of wastewater, its temperature, and composition [74]. The applied voltage and the characteristics of the ion exchange membranes also determined to a large extent the efficiency of the system [74].

Electrodialysis systems can produce very high-quality effluents with relatively low energy consumption, achieving 80–95% water recovery rates [75]. An electrodialysis system consumes approximately $0.49\,kWh/m^3$ at 1000 mg/l of TDS at 75% recovery and $1.75\,kWh/m^3$ at 5000 mg/L of TDS [73]. However, they are selective in their removal and therefore fail to remove colloids and organic matter, often making them uneconomic on their own. Furthermore, electrodialysis systems do not remove neutral toxic components such as bacteria and viruses, requiring posttreatment of the effluent [76]. In addition, electrodialysis operation cost can go above reverse osmosis when influent's TDS concentration exceeds 12,000 ppm [77].
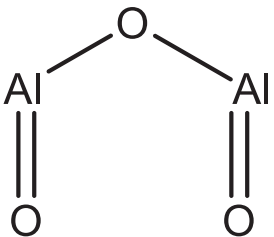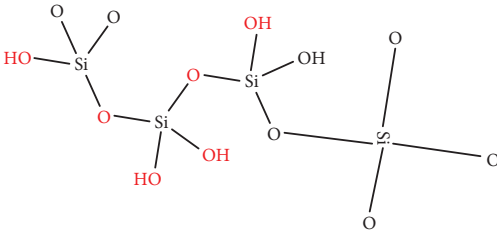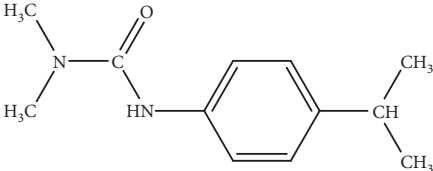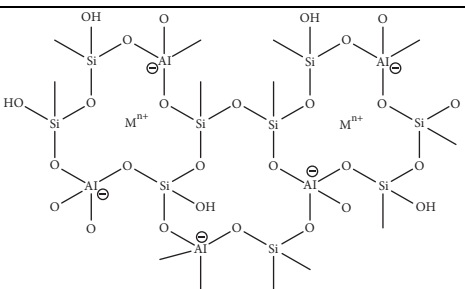
4. Adsorption

Adsorption process has been utilized in water purification systems extensively, making it one of the most used water purification techniques [78]. The adsorption process occurs physically through electrostatic charges or chemically through formation of bonds on the surface or the pores of porous solids in liquid or gaseous media [79]. In this regard, therefore, adsorption can be described as the process, whereby adhesion of atoms, molecules, or ions occurs in response to excess surface energy due to bond deficiency [80]. To efficiently remove contaminants, an adsorbent needs to possess suitable physicochemical characteristics. These include long service life, high adsorption capacity, high selectivity, and low-cost [81]. Surface functional groups, active surface, pore distribution, and pore diameter are important parameters when characterizing adsorbent materials [81].

4.1. Types of Adsorbents.

The most common types of commercial adsorbent currently in use include zeolites-based molecular sieves, polymeric adsorbents, activated alumina, activated carbon, silica gel, and carbon-based molecular sieves [82]. Most of the adsorbents like activated carbon and polymeric adsorbents are usually manufactured, while others such as clay occur naturally. Zeolite adsorbents can be synthesized or occur naturally. The structural properties of the adsorbents determine their applications [53, 81, 83–85]. Table 1 summarizes some applications of common adsorbents.

Adsorbents application and type is largely dependent on their specific characteristics. Synthetic adsorbents are currently most sought after due to their customizability at synthesis and their selectivity in adsorption [92–95]. With the world looking for affordable, renewable, and efficient adsorbent solutions, researchers are looking into utilizing agro-wastes and abundant resources like clay for adsorbent purposes.

4.2. Characteristics of Adsorbents.

For a material to be effective as an adsorbent for metal ions, it needs to exhibit some characteristics that fall into either physical or chemical characteristic groupings [85]. Physical characteristics include porosity, surface area, density, and particle size. Porosity refers to the total amount of space void available to the material. The more the pores, the higher the adsorption capacity of the material is [96]. Yakout [97] illustrates the increase in mesoporous pore increase in adsorption studies. A similar study by Tang et al. [98] reported higher Pb^{2+} and Cd^{2+} for the activated carbon adsorbent with a higher pore volume, agreeing with this observation. The rate of mass transfer is usually influenced by the external surface area [99]. External mass transfer occurs with the formation of a hydrodynamic layer covering the adsorbent, whereas internal mass transfer occurs through intraparticle diffusion. Efficient adsorption is highly dependent on the internal surface area and is responsible for material pore characterization as microporous, mesoporous, or macroporous. The total volume of pores available to an adsorbent material gives its adsorption capacity [97]. In an adsorptive study by

TABLE 1: Summary of applications of common adsorbents [83].

Adsorbent	Pore diameter (nm)	Structure	Applications	References
Activated alumina	8.096		Removing HCl gas from hydrogen Drying gases, transformer oils, and organic solvents Removing fluorine in alkylation processes	[86, 87]
Silica gel	2–11		Dew point control for natural gas Act as a desiccant Drying gases, organic solvents, etc.	[81, 88]
Activated carbon	0.54–0.59		Removing odors Purifying helium Usage in water purification systems	[89, 90]
Zeolites	0.3–0.8		Separation of oxygen from air Purifying hydrogen Recovering carbon dioxide Sweetening of sour gases and liquids	[81, 91]

Ouyang et al. [100], the synthesized adsorbent follows pseudo-first-order kinetic model in the adsorption of Pb^{2+}, Cd^{2+}, and Cu^{2+}. This results in the fact that the adsorption process is most likely a physisorption process. This adsorption process follows an external mass transfer phenomenon. In a different study, zeolites synthesized from natural kaolin were used in the adsorption of various metal ions, and the adsorption kinetic study revealed adsorptive energies below 40 kJ/mol, which indicated the physisorption process [101]. Similar findings were reported by Shehata et al. [102].

The chemical characteristics of an adsorbent involve the availability of surface-active functional groups to the material that can interact with contaminants and favorable surface chemistry [103]. Surface chemistry is the determinant of interactions between the adsorbent and the adsorbate, especially adsorption into oxidic sites [96]. In an investigation by Tran et al. [104], studying the effect of modification of the surface chemistry of zeolitic adsorbents on contaminant adsorption, it was reported that the modification of the Na of Y-zeolite improved its cation exchange capacity. Modifying it with surfactants opens the material to a wider range of adsorbates. In a similar study, the authors modified municipal sewage waste incineration fly-ash-based zeolite with Na_2PO_4 and reported 22 times higher adsorption compared to the unmodified zeolite [105]. Similar studies have reported enhanced metal ion adsorption on the modification of surface chemistry of various zeolite-based adsorbents [105–108].

4.3. Adsorbents in Water Treatment. Activated carbon (AC) has been in use for the adsorption of both inorganic and organic contaminants over the years. The selectivity to inorganic or organic compound adsorption depends on the material of origin and the process of activation [109]. Soft carbonaceous materials generally produce large-pored AC that are often applied in removal of organic compounds [110]. Harder materials produce AC with smaller pores often used in the removal of inorganic contaminants [111]. The process of activation can, however, alter the characteristics of the resultant AC [110]. Activated carbon is prepared from carbonaceous compounds such as wood, and agro-wastes achieve a high surface area and porosity for application in

heavy metal adsorption [85]. Activated carbon can be used in various forms ranging granulated form (0.6 – 4 mm granules), powdered form (44 μm), and fibrous structures with low hydrodynamic resistance [112]. Activated carbon has been documented to achieve a high contaminant removal efficiency of more than 94% for contaminant concentration of between 100 and 1600 μg/l with a carbon dose of approximately 1.25 g/l [113]. Activated carbon technology is limited by very high costs of production and use. Researchers circumnavigate this by sourcing cheaper material for the synthesis of activated carbon and/or modifying the surface chemistry of the material [112]. Nejadshafiee and Islami [114] modified activated carbon produced from pistachio shells with Fe_3O_4 nanoparticles and 1,4-butane sultone and reported high adsorption capacities for Pb^{2+} (147.05 mg/g), As^{2+} (151.51 mg/g), and Cd^{2+} (119.04 mg/g). In a similar study, Kyzas et al. [115] investigated the effect of nanobubbles on the adsorption of Pb^{2+} by activated carbon based on potato peels and reported almost equal adsorption of the metal ion by the modified carbon compared to the unmodified. However, the adsorption duration was boosted by over 300%, which indicated that the nanobubbles had a catalytic effect on the adsorption process.

Carbon nanotubes (CNTs) have one-dimensional tube-like structures resulting from rolled-up graphene sheets. They can be single-walled (SWCNT) or multiwalled (MWCNT) and contain a high surface area for contaminant adsorption. CNTs offer internal sites, interstitial channels, groove sites, and exterior surfaces as active adsorption sites making them excellent adsorbents [96]. Interactive forces due to carbon on the CNT surface cause challenges of aggregation, difficulty in manipulation, and poor dispersibility. Since the active sites on a CNT are found on defected segments of the structure, like pentagons on a body of hexagon structures, their interaction with other compounds in "raw" form is often limited [116]. They are modified by functionalization to enhance their interactions, using covalent (attached to CNTs skeleton) or noncovalent (functional groups coating the walls of CNTs) functionalized [117]. The process of functionalization is subject to the chemical and physical properties of CNT such as the nature of the CNT surface, particle size, and the chemical composition of the material [118]. In a study to compare adsorption performance of oxidized and double-oxidized MWCNTs, Rodríguez and Leiva [119] reported an increase in adsorption of Cu^{2+} (7.8–14 mg/g), Mn^{2+} (3.7–6.6 mg/g), and Zn^{2+} (2.7–4.0 mg/g). The authors reported that the adsorption followed the Langmuir's adsorption isotherm, which indicated that the adsorption process was a monolayer. The increase in adsorption was an indication of an increment in adsorption sites on the surface of the MWCNT for the double oxidized MWCNT. Other authors have reported similar findings on MWCNT oxidization modifications [120–122]. Polymers such as polydopamine [123] and polyethylenimine [124] have been utilized to functionalize MWCNTs to improve their heavy metal adsorption. High adsorption capacities with polydopamine functionalization have been reported as 318.47 mg/g for Cu^{2+} and 350.87 mg/g for Pb^{2+}.

$$M_{\frac{x}{n}}[\,(AlO_2)_x\cdot(SiO_2)_y\,]\cdot w\,(H_2O)$$
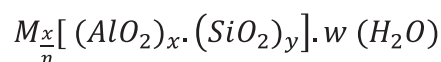
Figure 2: General formula of zeolite, adapted from Golbad [127].

Clay and clay-based compounds are other common adsorbents that have been extensively utilized in the removal of heavy metals from wastewater. We have recently published a review article discussing use of clay-based materials in heavy metal removal. The article can be accessed through [125].

4.3.1. Zeolites. Zeolites are crystalline, porous, and hydrated aluminosilicate minerals, characterized by specific molecular pore size [126]. When occurring naturally, they are found in temperatures often below 200°C in basaltic cavities, crystalizing due to hydrothermal alteration or diagenetic processes [126]. Zeolites possess three-dimensional structures that arise from polyhedral $[SiO_4]^{4-}$ and $[AlO_4]^{5-}$ polyhedral (Figure 2). They are capable of both facile and reversible cation exchange, acting as molecular sieves due to their tetrahedral structure, as shown in Figure 2 [128].

M represents a cation, with valence n, whose purpose is to balance negative charges due to aluminium tetrahedral, x and y are the stoichiometric coefficients of alumina and silica, w is the number representing the water molecules. M is often an alkali or an alkali Earth metal.

The crystalline structure gives them fascinating properties, such as shape selectivity, ion exchange, sorption capacity, catalytic activity, and host for advanced materials. The sorptivity of zeolites depends on the opening of the pores and the volume of the voids in the material. The ion exchange of zeolites depends on cation sites nature and how accessible they are for exchange [129].

In heavy metal adsorption studies, natural zeolites such as mordenite, chabazite, and clinoptilolite have been on major focus with performance comparative studies. However, the cation exchange capacity and heavy metal adsorption capacity of natural zeolites are predetermined and therefore limited by natural processes, leaving little room for modification. Synthetic zeolites show flexibility since their topology, pore distribution and size, and cation type in the zeolite framework, and the particle size can be controlled during synthesis [127, 130]. Framework and structure of basic zeolite elements is given in Figure 3.

The arrangement of atoms on the zeolitic molecular structure (Figure 3) gives the lattice a negative charge when Al^{3+} substitutes Si^{4+} in an isomorphous fashion [132]. The zeolite solid achieves electroneutrality through counteractions that reside in hydration water in the voids of the zeolite [131].

The framework of a zeolite describes the connectivity of the tetrahedral arranged atoms to achieve the highest form of symmetry. In describing the framework, a 3-letter code is assigned that is in accordance with the International Zeolite Association (IZA), and the codes are usually derived from the zeolite name, that describes the 'kind of material' [133]. For example, faujasite has the code FAU, and the MFI code represents zeolite Socony Mobil-Five (or ZSM-5). Common
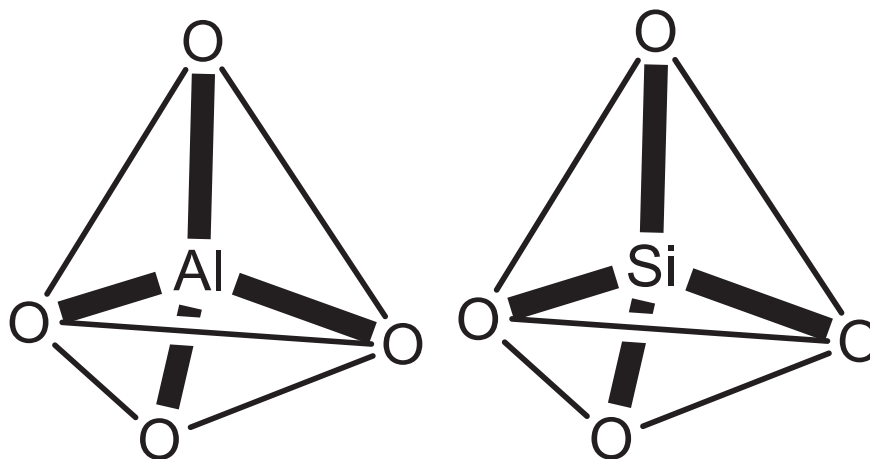
FIGURE 3: Sketch of the structure of the zeolite and $[AlO_4]^{5-}$ or $[SiO_4]^{4-}$ tetrahedral representation (adapted from [131]).

Double 4-ring

Double 6-ring

Four 5-ring unit

Pentasil unit

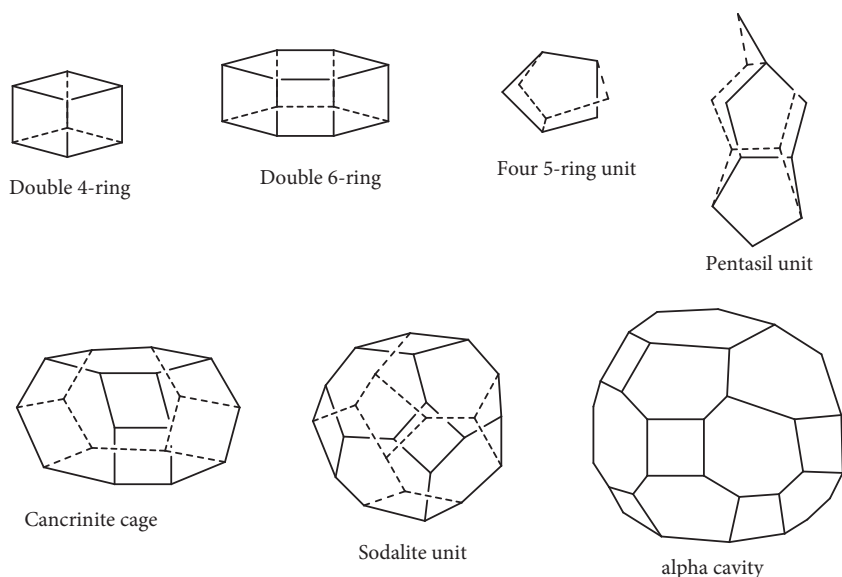Cancrinite cage

Sodalite unit

alpha cavity

FIGURE 4: Cavities and subunits common among framework types adapted from [128].

synthetic zeolite types include zeolite A, X, B, Y, and SZM-5, among others. In order to describe a zeolite structure, the framework is described first in terms of the dimensions of the channel system and the opening sizes of the pores. The ring size defining the pore characterizes the pore openings and usually designated the n-ring label, whereby n stands for the number of O- and T-atoms in a ring. Thus, an 8-ring framework has a pore width of about 0.41 nm and is considered microporous, 10-ring with a pore width and considered mesoporous, and 12-ring with 0.74 nm pore width and considered microporous [127]. A few structural features such as channels, cages, sheets, and chains are shared among zeolite frameworks as shown in Figure 4.

(1) Distribution and Occurrence of Natural Zeolites. Zeolites occur within different types of rocks, of differing ages and in diverse geological environments [134]. They are naturally formed as a result of a solid material reacting with its own pore water. Zeolites have been found to be deposited as

cavity fillings in altered volcanic rocks [135]. They have also been found in sedimentary rocks of marine origin, formed as a result of the alteration of volcanic glass [126]. Metamorphic rocks have also been reported to contain zeolites formed under extreme geothermal conditions at great depths [131]. The occurrence of some minerals in the zeolite group is summarized in Table 2.

According to Table 2, it can be seen that most rocks in which zeolites occur are generally volcanic and sedimentary rocks. When they occur in volcanic rocks, they occur as cavity fillings often as vapor or fluid deposition, while in sedimentary rocks, they are often alterations of volcanic glass [142].

(2) Properties of Zeolites. Zeolitic minerals exhibit adverse chemical and physical properties depending on their type. In terms of color, they can be transparent or appear in varying colors. In pure form, zeolites will often appear transparent or colorless and brownish reddish to greenish if they contain impurities [143].

TABLE 2: Summary of occurrence of some zeolites.

Zeolite mineral	Chemical formula	Occurrence	Reference
Alflarsenite	$NaCa_2Be_3Si_4O_{13}(OH) \cdot 2H_2O$	Syenitic pegmatite (Larvik, Denmark)	[136]
Amicite	$K_2Na_2Al_4Si_4O_{16} \cdot 5H_2O$	Basaltic rock (Howenegg, Germany)	[137]
Analcime	$Na(AlSi_2O_6) \cdot H_2O$	Basalts and phonolites (Catania, Italy)	[138]
Bikitaite	$LiAlSi_2O_6 \cdot H_2O$	Lithium-rich pegmatites (Bikita, Zimbabwe)	[139]
Boggsite	$Ca_8Na_3(Si, Al)_{96}O_{192} \cdot 70H_2O$	Porphyritic basalt (Goble Creek, Oregon, USA)	[140]
Brewsterite-Sr	$(Sr, Ba, Ca)[Al_2Si_6O_{16}] \cdot 5H_2O$	Basalts and schists (Strontian, Scotland)	[141]

Most zeolites exhibit density in the range 2–2.3 g/cm³, although it is not uncommon to observe density values ranging 2.5–2.8 g/cm³ especially those with abundance of Ba atoms, like Brewsterite. Bulk specific gravity has been documented to range between 0.80 and 0.90 g/cm³ [144].

Zeolites exhibit massive ion exchange capacities. The cation exchange capacity (CEC) of zeolite minerals is often in the range 200–300 cmol/kg, although it can reach up to 400 cmol/kg. The value of the CEC is dependent upon factors such as the pH, temperature electrolyte concentration in the solution, structural characteristics of the zeolite, dimensions and the shape of new cation, and the anionic charge density in the framework, among others [145].

Zeolites also exhibit a unique property and adsorption selectivity, which is greatly defined by the diverse ions and molecules with varying sizes trapped within the zeolite pores. This parameter is responsible for the novel molecular filtration capabilities of zeolite, which are dependent on the structure of the zeolitic crystal and the separation capacity that is based on polarity, shape, or size, thus making the zeolite a selective adsorbent [144].

The catalytic properties of zeolites arise in response to the distribution of various acidic regions in the crystalline lattice of the zeolite. In addition to this, the size of both the internal cavities that act as reaction chambers and the surface resources have an effect on the catalytic activity of zeolites. Any zeolite is still able to affect reaction selectivity through molecular traffic control, transition state selectivity, or selectivity of the product or the reaction [146].

Other important properties of zeolites include thermal stability that is about 1000°C, structural stability against acid, alkaline and radioactive environments, refractive indices ranging 1.47–1.52, and water adsorption capacity in the range 45–75 ml/100g [143].

Generally, a zeolitic material will be adverse in color depending on impurity levels and show a density in the range of 2–2.8 g/cm³ with specific gravity values ranging 0.80–0.90 g/cm³. The material will also portray high CEC values of up to 400 cmol/kg and great selectivity in its ion adsorption [147–149].

5. Synthetic Zeolites

Naturally, zeolites have been formed out of the reaction of volcanic ash and basic lake water in a process lasting thousands of years [150]. Synthetic zeolites are fabricated in a simulated hydrothermal process, temperature, and pressure using synthetic silicates or natural materials [151]. Appropriate equipment, energy, and uncontaminated substrates are required to achieve quality synthetic zeolite. In this regard, it is important to note that the synthesis reactions can incur costs that directly influence the price of the product, in which case would be uneconomic. The recent focus in the field of synthetic zeolites is, therefore, reaction cost reduction [152]. This is achievable by using waste or natural raw materials. High silica natural materials such as diatomite, halloysite, clay minerals, pumice, and volcanic glasses have therefore been in the spotlight for zeolite synthesis [153].

Depending on the silica content, synthetic zeolites are distinguished as low silica (with Si/Al ~ 1–1.5), intermediate silica (with Si/Al = 2.5), and high silica (with Si/Al > 10), a parameter that directly reflects the specific properties of the zeolite [154]. A low Si/Al ratio translates to increased ion exchange capacity for the material and high adsorption capacity towards polar molecules. A high Si/Al ratio translates to high catalytic activity, hydrothermal stability, and increased hydrophobicity [144].

5.1. Synthesis of Zeolites

5.1.1. Factors Affecting Zeolite Synthesis.
To achieve high-quality zeolites, years of practical experience have outlined some important factors to consider, namely, the silica to alumina ratio, reactants composition, aging, temperature and time, crystallization, and alkalinity [155]. The composition of the reaction mixture, which incorporates the silica to alumina ratio, the inorganic cations, and OH⁻ions, requires close attention to achieve highly customized zeolite compounds [156]. Increasing the Si/Al ratio affects the material's physical properties, while OH⁻ affects the mobility of the silicates from the solid phase to the solution, thus affecting nucleation times [157]. The inorganic cation has the most important role in balancing the charge of the framework and acts as agents directing the structure, thereby directly affecting the product yield and crystal purity. In the synthesis of hierarchical Y zeolites, Feng et al. [158] studied the effect of NH_4HF_2 etching on the formation of zeolitic crystals with X-ray diffraction (XRD) data showed enhanced peaks for NH_4HF_2-etched zeolite, which demonstrated the effect of reaction mixture composition on zeolite synthesis.

The nature of reactants and the level of their pretreatment is another important factor. Since the synthesis process involves the utilization of both organic and inorganic precursors, inorganic precursors produce more hydroxylated surfaces, as organic precursors incorporate metal ions into

the network [159]. In the synthesis of zeolite W, the researchers used natural zeolite waste. With thermal treatment at 400–900°C, the crystalline zeolite formed remained below 36.5%. However, when they tried alkali fusion treatment at 600°C, a larger amount of Al species was activated and less than 40% of silica species. In this way, more zeolite W crystals were formed [160].

Temperature affects nucleation and rate of crystallization in the synthesis of zeolites. The crystallization rate is usually directly proportional to the temperature change. The nucleation rate, on the other hand, exhibits an inverse proportionality to the temperature change [161]. Zhao et al. [162], in a study to characterize the synthesis of high silica Y zeolites, investigated the effect of precursor pretreatment in the zeolite synthesis with NMR data showing higher zeolite crystal formation for precursors aged at low temperatures.

Reaction time is a factor that is often managed by the crystallization process. The crystallization is adjusted to minimize other phase production, while minimizing the time required to achieve required crystalline phase [163]. In a study investigating the synthesis of zeolite SSZ-13 from coal gangue, the researchers reported gradual increase in synthesis time up to 36 hours [164]. In a similar study, Krachuamram et al. [165] investigated the effect of aging time on crystallites formation and reported an optimum aging time of 3 days for NaX zeolites synthesis.

In summary, the composition of the reaction mixture determines the texture and often the duration of zeolite synthesis. Pretreatment of the precursors can determine the failure or success of zeolite formation. The temperature is often defined by the synthesis method, but plays a role in the nucleation of the zeolite crystals. The reaction time needs to be closely monitored as different zeolites achieve maximum formation within certain time ranges, beyond which crystals degrade.

5.1.2. Methods Applied in the Synthesis of Zeolite.
Zeolites are synthesized by heating aluminosilicate raw materials for a period of time that spans hours or days (depending on the type of the raw material and the process conditions) in the presence of high pH solutions [153]. Common methods currently applied in zeolites synthesis include hydrothermal synthesis [166], microwave-assisted synthesis method [167], molten salt [103], activation of alkali fusion activation [168], and synthesis through dialysis [153].

The hydrothermal synthesis method usually simulates the natural conditions through which rocks containing zeolites are formed. Hydrothermal temperatures of 80–350°C are involved in treating aluminosilicate raw materials in an alkaline solution with pH above 8.5 [169]. The reactions that occur (dissolution, gelatinization, condensation, and crystallization) are conducted in an autoclave at elevated pressure [170]. Careful alteration of process parameters gives products with desired properties [153]. Garcia-Villén et al. [166] used the hydrothermal synthesis method to synthesize zeolite using waste from sanitary ware. Researchers used 5M NaOH alkaline solution at temperatures 100, 150, and 200°C for up to 30 days and reported the

transformation of quartz and mullite minerals to zeolite. Luo et al. [171] synthesized needle-like zeolites from metakaolin using the same method for utilization in the removal of organic and heavy metal contaminants. Hydrothermal synthesis is a common method in the synthesis of zeolites. It, however, suffers limitations as high cost, especially with the use of high-pressure autoclaves and produces excessive waste, making it environmental unfriendly [172].

Molten salt method for zeolite synthesis was proposed to address the shortcomings of hydrothermal method such as high ratio of solution to solid and low product yields [173]. In the molten salt method, synthesis takes place under molten conditions without the addition of water. The high-silica raw material, a salt, and a convenient alkaline solid are finely ground and melted at convenient temperatures for extended periods of time. They are then cooled, crushed and washed. Common bases used include KOH, NH_4F, and NaOH [174, 175]. Common salts used include $NaNO_3$, KNO3, and NH_4NO_3. This method was often used to synthesize fly ash-based zeolites [176–178]. Since the molten salt method required high temperatures for the synthesis of zeolites, the most serious limitation associated with the method was the high energy consumption rates, often worsened by the duration of synthesis of the material [179]. Recently, authors are using modifications of the method to reduce energy consumption cost through sub-molten salt (SMS) synthesis. In SMS technology, high-alkaline (above 50%) and high-boiling-point precursors are used to ensure reaction conversion and mass transfer while keeping temperatures low, under ambient pressures [180]. Meng et al. [181] used the SMS method in precursor treatment using 75% alkaline solution and an alkali to ore ratio of 3.5 : 1 at a temperature of 200°C, during the synthesis of zeolite W from potassic rocks. The resulting material achieved an exchange capacity of 156.8mgK$^+$/g and 30.39mgK$^+$/g in KCl and simulated sea water solutions, respectively. Similarly, Krisnandi et al. [182] synthesized ZSM-5 zeolite crystals from natural zeolites using the fragmented SMS method. Natural zeolite was pretreated at 250°C in alkaline solution. The resulting material showed the BET surface area of 262 m^2/g, which is typical for a microporous zeolite.

Microwave irradiation is a modern green technique that has been used in the fabrication of zeolites. Different ratios of aluminium to silica sources and structure directors are usually mixed uniformly and irradiated by microwaves in autoclaves [183]. Parameters such as the size and shape of the autoclave, reaction time, and power and temperature of the microwave are adjusted carefully to affect the morphology, as well as the structure, of the zeolite [184]. Majdinasab et al. [185] used the microwave radiation technique in the synthesis of zeolites from pulverized waste glass cullet in comparison with convection heating. The authors reported microwave radiation being more efficient, achieving 60% maximum relative crystallinity of the zeolite. Similarly, Wong et al. [186] successfully synthesized nanocrystalline F-type zeolite using an organic template-free system by using rice husk ash as the silica source under microwave irradiation.

5.1.3. Agro-Waste in Zeolite Synthesis.

Rice husk ash (RHA) has been extensively investigated as a potential silica source for the synthesis of zeolites. Many methods have been proposed for the extraction of silica from RHA, including biological treatment, chemical treatment, hydrothermal-baric, and thermal methods at elevated temperatures of 400–700°C [156, 187]. Bohra et al. used RHA alongside aluminium foil as precursors for NaA and NaP zeolite synthesis in two different studies showing a greener approach in the synthesis of zeolites [188]. Most researchers have focused on RHA as an agro-waste source of silica as seen in works of Mallapur et al. [189]; Bohra et al. [190]; Alaba et al. [191]; and Min et al. [156]; among others.

Sugarcane bagasse fly ash (BFA) has also been utilized as a low-cost precursor for zeolite synthesis. BFA is a rich source of alumina, and silica minerals needed to achieve high CEC zeolitic materials. Oliveira et al. [192] synthesized calcined sugarcane BFA and zeolite NaA using the hydrothermal synthesis method for application in the removal of copper ions from wastewater.

Several other agrochemicals that have been utilized in the synthesis of zeolites are summarized in Table 3.

5.1.4. Clays in Zeolite Synthesis.

Kaolin-based zeolites have been synthesized in an effort to achieve affordable zeolitic products. Kaolin clay mineral, illustrated in Figure 5, consists of silica tetrahedral joined to alumina octahedral in the ratio of 1:1 through shared oxygen atoms. Kaolin-based zeolites will often have Ca, Mg, Fe, Ti, etc., contaminants originating from natural kaolin, which may affect the properties of the final product [199]. Kaolin is often calcined to temperatures ranging from 550 to 950°C to achieve reactive metakaolin for utilization in the synthesis [163].

Fortunately, kaolinite is not the only type of clay mineral utilized in the synthesis of zeolites. Ltaief et al. [200] synthesized faujasite zeolite from Tunisian illitic clay exhibiting hierarchical porosity. Researchers used the molten salt synthesis method using NaOH in muffled furnace. Zeolite crystallization occurred at 60°C in 24 hours. The resultant material was used in adsorption of various heavy metal ions, and removal capacities were reported to be 126 mg/g (Cu^{2+}), 125 mg/g (Co^{2+}), and 98 mg/g (Cr^{3+}). These findings were higher than the commercial faujasite adsorption capacities for the respective metal ions as 120 mg/g, 118 mg/g, and 91 mg/g. This study illustrated a low-cost zeolite material with better efficiency in heavy metal adsorption.

A study by Medina-Rodríguez et al. [201] used Ecuadorian clay to synthesize zeolite X through alkaline fusion and hydrothermal treatment. Sodium aluminate and NaOH were used to fine-tune the properties of the zeolite at synthesis. The resulting zeolite X was reported to have a specific surface area of 376 m^2/g, which was 30 times higher compared to clay (12 m^2/g). The zeolite was used in the removal of Pb^{2+} and achieved an adsorption capacity of 24 mg/g, much higher compared to that of clay (13 mg/g).

Moneim and Ahmed [202] synthesized low silica NaX-Faujasite zeolite from different types of Egyptian clays (kaolinite, smectite-kaolinite, and smectite-rich clays) using a combination of hydrothermal synthesis and alkali fusion methods. Crystallization conditions were 100° C and 48 hours for smectite-kaolinite clay and 72–96 hours for the kaolinite and smectite-rich clays. The authors reported that the smectite-kaolinite clay had better crystallization rates compared to the rest. Zeolite was applied to remove Cr^{3+}, Ni^{2+}, and Mn^{2+}, and the percentage removal was reported to be 100%, 80%, and 75%, respectively.

Gaidoumi et al. [203] reported the successful synthesis of zeolite HS by using natural pyrophyllite clay as raw material. The clay was treated with alkaline, and the resultant material is characterized by X-ray fluorescence and Fourier transform infrared, among other techniques. The authors reported that the resultant zeolite was nearly pure. Aghaei et al. [204] alkali-fused the same clay to synthesize zeolite Y and reported improved acidity and textural properties compared to commercial zeolite Y. Foroughi et al. [205] combined illite, pyrophyllite and kaolinite clays to synthesize zeolite A through fusion technique and reported mesoporous zeolite structure which contained a surface area of about 59.6 m^2/g and an average pore size of 8 nm.

Joseph et al. [206] synthesized multiple zeolites using vermiculate-kaolinite clay through the alkaline fusion method. The clay mixture achieved the synthesis of faujasite-based zeolite without pretreatment. On thermal activation, the clay was able to produce gismondine zeolite GIS-NaP1. When it was pretreated by acid leaching, the clay produced mixed-phase quartz and Na-P1 zeolites.

6. Characterization of Zeolites

6.1. Scanning Electron Microscopy (SEM) and Energy Dispersive Spectroscopy (EDS).

Scanning electron microscopy technique is used to analyze surface morphology and topology of zeolitic materials by focusing a beam of low energy electrons on the sample. Interactions of the beam and the material led to emission of electrons and photons that are detected and take part in the formation of SEM image [207]. EDS is useful in the chemical analysis of materials. It is typically equipped with SEM and makes use of X-rays to identify the chemicals present in a sample [208]. Studies in which SEM analysis has been utilized in zeolite characterization are summarized in Table 4.

6.2. Brunauer–Emmett–Teller (BET) Analysis.

BET analysis is an important analytical technique in the characterization of zeolites as it gives data regarding adsorption mechanism of the material. By using probing gases, the BET theory seeks to provide information on the specific surface area of multilayer pore systems to understand the adsorptive characteristics of a material [213]. Nitrogen is a common probe gas, although others can be used, as long as they do not chemically react with the surface of the material analyzed [214]. Previous studies whereby BET analysis has been utilized in zeolite characterization are summarized in Table 5.

TABLE 3: Other wastes in the synthesis of zeolites.

| Waste material	Zeolite formed	Synthesis method	Product yield (%)	Reference
Coal combustion fly ash	Analcime, faujasite, gismondine	Hydrothermal treatment	70–80	[193]
Municipal solid waste fly ash and waste bottle powder	Perlialite, zeolite A and Y	Fusion hydrothermal	—	[194]
Volcanic ash	Na-mordenite	Hydrothermal synthesis	80	[195]
Municipal solid waste	Clinoptilolite	Hydrothermal conversion	69	[196]
Blenod fly ash	Na-X faujasite	Hydrothermal conversion	20–25	[197]
Paper sludge ash	Na-PI zeolite	Hydrothermal synthesis	—	[198]
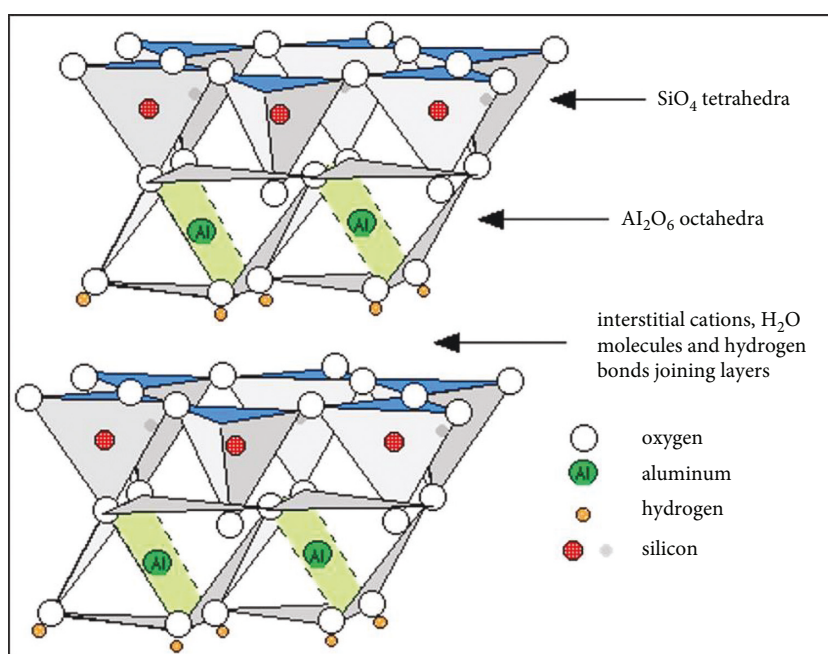
FIGURE 5: Structure of kaolinite (adapted from [199]).

6.3. X-Ray Diffraction (XRD).

XRD technique is extensively used in the analysis of crystalline compounds, more so in the characterization of zeolite compounds. Data resulting from XRD gives insight into the texture, phase, grain size in average, crystal defects, and strain, among others. This is usually possible through the interference of X-ray beams by lattice planes available in a sample [219]. Crystalline samples are identifiable by referencing a standard database for XRD patterns [220]. Previous studies in which XRD analysis has been used in zeolite characterization are summarized in Table 6.

6.4. Fourier Transform Infrared (FTIR) Spectroscopy.

FTIR spectroscopy identifies materials by analyzing the vibrations depicted by chemical bonds within a material's molecular structure [222]. Different chemical structures absorb infrared radiation at different wavelengths giving rise to a peak and therefore identification [223]. The chemical environment is important for understanding the functional groups in the material [224]. FTIR analysis is necessary to understand how effective the zeolite is in the removal of heavy metals. FTIR spectroscopy is able to analyze mid-IR region between 5000 and 400 cm^{-1} and near-IR region between 10,000 and 4000 cm^{-1} [225]. Several studies have utilized FTIR analysis in zeolite characterization with different chemical groups as summarized in Table 7.

6.5. Thermogravimetric Analysis (TGA).

TGA's sole purpose is identification of a material's thermal stability and percentage of volatile compounds in its structural composition, usually through monitoring the change in the material's weight as heating occurs in a predetermined rate [230]. In zeolite studies, TGA is useful in analysis of a zeolite's amount of pore water. Ezzeddine et al. [231], in a study to utilize zeolite NaX in heavy metal adsorption, used the TGA technique to investigate the water content and absence of the

TABLE 4: Summary of SEM analysis of zeolites.

Zeolite	Raw material	Synthesis method	Observations	References
FAU-type zeolite	Coal fly ash	Alkaline fusion + hydrothermal treatment	High water content and longer ageing time resulted to better defined zeolite	[209]
K-ZFA Zeolite	Coal fly ash	Hydrothermal alkaline treatment	The material showed low degree agglomeration	[210]
Zeolite A	Natural Sudanese montmorillonite clay	Alkali fusion	Uniform particle morphology. Small particle size in the range 3.72–8.61 μm	[211]
Magnetic NaA Zeolite	Natural kaolin	Hydrothermal treatment	Crystals with the same cubic morphology and almost same diameter ($2\,\mu$m)	[71]
Cancrinite	Natural Tunisian clay	High pressure hydrothermal treatment	Symmetric hexagonal needlelike shapes	[212]

organic template used during synthesis. Authors reported about 26% water loss between 25 and 900°C. Similarly, in a study conducted by Oliveira et al. [192], weight loss was initially observed up to 200°C and attributed to water loss. Additional weight loss was observed between 350 and 580°C and attributed to elimination of carbon and other organic residues. Other works utilizing TGA analysis have been summarized in Table 8.

7. Adsorption Studies

7.1. Adsorption Isotherm Models. Adsorption isotherms show the relationship between the quantity of the solute that has been adsorbed and the solute's concentration in the liquid phase [131]. Understanding this relationship is important to examine the performance of zeolites in heavy metal adsorption. Different models have been proposed and used over the years to understand this behavior. Some of these methods are discussed.

The Langmuir adsorption isotherm is modeled with the assumption that the maximum adsorption corresponds to saturation of the monolayer adsorbate surface. This implies that all sites of adsorption are identical, and the adsorption energy is constant. The Langmuir isotherm is therefore described by the linear equation [234].

$$\frac{C_e}{q_e} = \frac{1}{Q_0 b} + \frac{C_0}{Q_0},\tag{2}$$

where q_e represents the quantity of adsorbed metal ion in (mg/g), C_e as the residual ion concentration at equilibrium, and Q_0 and b, Langmuir's constants for sorption capacity and energy, respectively. b should vary with temperature since it is a representation of the enthalpy of adsorption [131].

The Freundlich isotherm is structured with the assumption that surface adsorption energies are irregular, implying heterogenous nature of adsorption [235]. This model can therefore be described by

$$q_e = K_f C_e^{1/n},\tag{3}$$

where q_e represents solute's adsorption per unit mass of the adsorbent at equilibrium in mg/g, C_e is residual ion concentration in the liquid phase at equilibrium, and K_f is the Freundlich constants determined by the conditions of the experiment [131]. The equation can be rewritten in linear form as

$$\log Q_e = \log K_f + \frac{1}{n}\log C_e.\tag{4}$$

When the value of $1/n$ falls below 1, this is an indication that the adsorption is heterogenous. Values near or equal to 1 indicate a material exhibiting somewhat homogeneous binding sites in relation to its porosity [236]. The utilization of these models in the adsorption analysis of some zeolites has been summarized in Table 9.

Lesser common isotherm models in zeolite metal ion adsorption studies such as Dubinin–Radushkevich (D-R) and Temkin isotherm models exist. D-R isotherm assumes filling of pores in the adsorption process in a multilayer character, involving van der Waals forces [234]. This model is often applied in the expression of Gaussian energy of adsorption distribution upon heterogenous adsorptive surface [243]. It is, however, unrealistic at low pressures since under such conditions, it does not follow Henry's laws. It is therefore most suitable for intermediate adsorbate concentrations [244]. Its best application in metal ion adsorption is differentiation between physical or chemical adsorption mechanism of adsorbates. D-R is described as follows [30]:

$$\ln Q_e = \ln Q_m - \beta E^2,\tag{5}$$

$$E = RT\ln\left(1 + \frac{1}{C_e}\right),\tag{6}$$

$$E = \frac{1}{\sqrt{2B}},\tag{7}$$

where e is Polanyi's constant, β is D-R constant, R is the gas constant, T is the absolute temperature in Kelvin, and E is the mean adsorption energy.

Temkin adsorption isotherm considers the indirect effect multiple adsorbents might have on each other (adsorbent/adsorbent interaction), upon the process of adsorption. This isotherm is governed by the assumption that the adsorption heat (ΔH_{ab}) of all interacting species decreases with increase

TABLE 5: Summary of BET analysis of zeolites.

Zeolite	Synthesis method	Observations	References
Zeolite A	Hydrothermal synthesis	An increase in pore size was observed compared to fly ash	[215]
Zeolite NaA	Hydrothermal synthesis	Mean surface area found to be 46.6 m^2/g	[216]
Clinoptililite	Ultrasonic-assisted preconcentration	Material identified as nanoporous	[217]
Zeolite X	Hydrothermal synthesis	Pore volume observed to be 0.22 cm^3/g and 260 m^2/g BET surface area	[218]

TABLE 6: Summary of the XRD analysis of zeolites.

Zeolite	Synthesis method	Observations	References
Clinoptililite	Ultrasonic-assisted preconcentration	Pore closure reduces peak intensity on modification	[217]
Zeolite X	Hydrothermal synthesis	Rietveld calculations shown 75% zeolite content	[218]
Zeolite A	Hydrothermal synthesis	Rietveld calculations shown 70% zeolite content	[218]
Zeolite ZSM-5	Hydrothermal treatment	The increase in nucleation period favored the formation of zeolite crystal	[221]

TABLE 7: Summary of FTIR analysis of zeolites.

Zeolite	Synthesis method	Observations		References
		Wavelength (cm^{-1})	Group or Reason	
Needle-like nanozeolite	Hydrothermal synthesis	3400	O-H stretch	[171]
		1640	Zeolitic water influence	
Hydroxy-sodalite/ cancrinite	Hydrothermal alkali activation	1400–400 (disappear)	Si-O, Si-O-Al vibrations	[226]
		4000–3500 (disappear)	-OH vibrations	
ZIF-8	Solvothermal synthesis	421	Zn-N	[227]
		692	Co-N	
		755	CN	
		1100–1310	C = N	
		1577	C = C	
NaP zeolite	One step hydrothermal synthesis	1008 and 735	Si-O or Al-O assymetric stretching	[228]
		690	Symmetric stretching of Si-O or Al-O symmetric stretching	
		600	Double ring in NaP	
		435	Si-O or Al-O bending	
Phillipsite zeolite	Hydrothermal synthesis	439.19	O-Si-O	[229]
		607.47	Si-C	
		693.06	Mn-O	
		1026.96	Assymetric Si-O-Al	
		1638.92	H-O-H or C = C	
		3435.81	Si-OH	

in surface coverage. This model is therefore only valid for intermediate adsorbate concentrations [234]. It is given by

$$Q_e = \frac{RT}{b} \ln K_t + \frac{RT}{b} \ln C_e, \qquad (8)$$

where b (j/mol) and Kt (L/g) represent Temkin constants, calculated from the slope and intercept of the plot of Q_e versus ln Ce, respectively [244].

Most zeolite-based adsorption isotherms follow Langmuir model according to Table 9. This translates that the metal ion adsorption is a monolayer adsorption, according to the high R^2 values. The few that follow Freundlich

isotherm model such as Cu and Cd adsorption by fly-ash synthesized zeolite X [239] imply a multilayer adsorption criterion.

7.2. Adsorption Kinetics. The pseudo-first-order (PFO) model, first described by Lagergren, is described by the linearized equation [245].

$$\ln(q_e - q_t) = \ln q_e - k_1 t, \qquad (9)$$

where q_t is adsorbed adsorbate at time t in mg/g, q_e is adsorption at equilibrium in mg/g, and k_1 is rate constant per minute. To determine the value of k_1, a plot of $\ln(q_e - q_t)$ against t is drawn.

TABLE 8: Summary of the TGA analysis of zeolites.

Zeolite	Observations (%)			References
	Percentage loss (%)	Temperature	Interpretation	
Faujasite-type zeolite	1.43	110°C	Surface water loss	[232]
	3.73	200°C	Internal water desorption	
Nanoclinoptilolite	2	—	Surfactant adsorption into sample	[233]
Nax-zeolite	26	200°C	Physisorbed water molecules	[231]
Needle-like nanozeolite	14	100–175°	Zeolitic water	[171]

TABLE 9: Summary of adsorption isotherms on synthetic zeolites derived from agro-wastes and clay.

Zeolite	Raw materials	Metal ion	Langmuir model		Freundlich model		References
			q_e (mg/g)	R^2	K_f (mg/g)	R^2	
Zeolite X	Ecuadorian clay	Pb^{2+}	131.6	0.994	31.33	0.977	[201]
Zeolite NaA	Bagasse ash	Ca^{2+}	555.54	0.987	2.24	0.9986	[237]
ZSM-5	Chlorite clay	As^{5+}	411.41	0.9907	74.63	0.9043	[238]
		Pb^{2+}	546.25	0.9921	653.15	0.7300	
Zeolite X	Coal fly ash	Ni^{2+}	1.136	0.8348	0.22	0.5669	[239]
		Cd^{2+}	1.795	0.5600	0.23	0.8077	
		Cu^{2+}	3.209	0.9890	1.65	0.9954	
NaA zeolite	Oil shale ash	Cu^{2+}	156.74	0.998	87.07	0.979	[240]
		Ni^{2+}	53.02	0.996	27.42	0.984	
		Pb^{2+}	224.72	0.978	91.34	0.938	
		Cd^{2+}	118.34	0.993	62.91	0.768	
Linde F (K) zeolite	Fly ash	Cu^{2+}	59.9	0.9763	66.8	0.0691	[241]
		Cd^{2+}	118.6	0.9567	1.42	0.7002	
		Pb^{2+}	476.1	0.9864	248.5	0.8149	
Zeolite 4A	Recycled coal fly ash	Co^{2+}	13.72	0.998	6.66	0.959	[242]
		Cr^{3+}	41.61	0.998	28.47	0.850	
		Cu^{2+}	50.45	1.000	37.11	0.974	
		Zn^{2+}	8.96	0.997	6.27	0.834	
		Ni^{2+}	30.80	0.945	18.47	0.623	

The pseudo-second-order (PSO) model has the assumption that solute adsorption is proportional to active sites on the adsorbent. Therefore, the rate of reaction is dependent on solute amount on the surface of the adsorbent. The PSO equation is illustrated as follows:

$$\frac{t}{q_t} = \frac{1}{k_2 q_e^2} + \frac{t}{q_e}, \tag{10}$$

where k_2 is a PSO rate constant. Applications of these modes in adsorption studies for synthetic zeolites are summarized in Table 10.

Other lesser common kinetic models in the adsorptive studies of metal ions in zeolite materials include intraparticle diffusion and Elovich models. Intraparticle diffusion model is common for a process whereby there is an increase in the rate of adsorption with increase in temperature, common in chemical adsorption processes. This model is illustrated by

$$Q = K_p \sqrt{t} + C, \tag{11}$$

where K_p and C are intraparticle diffusion constants. A plot of Q versus $\sqrt{t}$ is used in estimation of the diffusion process. If the plot is observed as a straight line, the adsorption is predicted to involve at least two stages of intraparticle

diffusion. This model can also be used to predict the thickness of the interface between the adsorbate and adsorbent [30].

Elovich model, given in equations (12) and (13) [30], is generally applicable to heterogenous-based chemisorption process, and the rate of desorption is negligible. This model is often used in the prediction of surface diffusion and mass and the activation or deactivation energy of an adsorbent [251].

$$Q = \frac{1}{\beta} \ln\left(t + \frac{1}{\alpha\beta}\right) - \frac{1}{\beta} \ln(\alpha\beta). \tag{12}$$

If $t \gg 1/\alpha\beta$, then

$$Q = \frac{1}{\beta} \ln(\alpha\beta) + \frac{1}{\beta} \ln(t), \tag{13}$$

where β and α are Elovich constants estimated from the plot of Q versus $\ln(t)$.

7.3. Thermodynamics of Adsorption. An adsorption process is largely affected by the temperature of the reaction medium. Thermodynamic studies are used focused on studying the behavior of the adsorbent efficiency at different temperatures by analyzing Gibb's free energy, enthalpy, and entropy of the reaction. The formulae used for this analysis are [53]

TABLE 10: Summary of adsorption kinetics on synthetic zeolites.

Zeolite	Raw material	Metal ion	Pseudo-first order		Pseudo-second order		References
			q_e	R^2	q_e	R^2	
ZSM-11	Rice husk ash	Pb^{2+}	1.4754	0.8503	3.3367	0.6912	[246]
		Zn^{2+}	1.0859	0.9929	1.7050	0.9662	
Zeolite A		Co^{2+}	65.28	0.9418	89.30	0.9529	
	Rice hush and aluminium cans	Cu^{2+}	65.23	0.9286	94.57	0.9565	[247]
Faujasite		Co^{2+}	62.14	0.9518	83.06	0.9566	
		Cu^{2+}	67.16	0.9268	92.03	0.9451	
Merlinoite	Sugarcane bagasse ash and kaolin	Pb^{2+}	127.17	0.8430	250.0	0.9999	[248]
Linde F (K)	Fly ash	Cu^{2+}	3.2319	0.8271	21.598	0.9983	[249]
		Cd^{2+}	1.6945	0.9867	22.221	0.9998	
		Pb^{2+}	2.098	0.9337	49.751	0.9982	
		Ni^{2+}	1.9823	0.8561	12.821	0.9998	
Zeolite NaP	Aluminium and fumed silica wastes	Ni^{2+}	45.15	0.8841	45.15	0.9846	[250]
		Cu^{2+}	66.75	0.8858	66.75	0.9934	

TABLE 11: Summary of adsorption thermodynamics on synthetic zeolites.

Zeolite	Raw material	Metal ion	T (K)	ΔG^0 (kJ/mol)	ΔH^0 (kJ/mol)	ΔS^0 (kJ/mol)	References
Zeolite Na-P1	Coal fly ash	Cr^{3+}	298	164			[252]
			308	165	23	−85	
			318	166			
Zeolite X	Raw municipal bio-slag	Cs^+	288	14.482			[253]
			298	14.272	20.53	0.021	
			308	14.062			
11Å-tobermorite	Coal fly ash	Cu^{2+}	298.15	4.368			[254]
			318.15	4.906	−1.090	−9.047	
			338.15	5.439			
		Pb^{2+}	298.15	4.342			
			318.15	4.923	−2.760	−5.277	
			338.15	5.683			
Zeolite Y	Fly ash	Cu^{2+}	301.15	−7.67			[255] bohr
			318.15	−8.90	14.14	72.43	
			338.15	−10.35			
		Ni^{2+}	301.15	−7.48			
			318.15	−8.86	16.94	81.08	
			338.15	−10.48			

$$K_d = \frac{C_A}{C_B}, \tag{14}$$

$$\Delta G^0 = -RT \ln K_d, \tag{15}$$

$$\ln K_d = \frac{\Delta S^0}{R} - \frac{\Delta H^0}{RT}, \tag{16}$$

where K_d is the constant of thermodynamic equilibrium, R is gas constant, T is the absolute temperature, and C_A and C_B are the concentrations of the adsorbate on the adsorbent and residual concentration at equilibrium, respectively [53].

An endothermic adsorption is given by a positive enthalpy value. A negative Gibb's free energy value implies thermodynamically spontaneous and sustainable at diverse temperatures. A positive entropy value gives an insight that there is randomness at the liquid-solid interface in the adsorption [53]. Thermodynamic studies on various synthetic zeolites are summarized in Table 11.

From Table 11, it can be inferred that the majority of zeolites give a positive Gibb's free energy value. This implies that, for the most studies summarized, the adsorption of the heavy metals is not thermodynamically spontaneous and therefore not diverse over a large range of temperatures. Zeolite Y, however, synthesized by Liu et al. [255] differed and gave negative Gibbs free energy for both copper (II) and nickel (II) ions adsorption. This implies that the adsorption is feasible over a range of temperatures and therefore sustainable. Zeolites Na-P1 [252], X [253], and Y [256] give positive enthalpy values. This implies endothermic adsorption process (physisorption). The negative enthalpy of 11Å-tobermorite [254] zeolite implies an exothermic adsorption process, which implies a chemisorption process in

the metal ions adsorption. Zeolite X and Y give positive entropy values, while 11Å-tobermorite and Na-P1 give negative values for the metal adsorption processes. A positive entropy value implies increased randomness at the solid-liquid interface, and thus, high metal ion adsorption is expected in such systems.

8. Conclusions

Although several methods exist for removal of heavy metals from wastewaters, heavy metals in waters still pose a global health concern. We therefore conclude the following:

(1) Most low- and middle-income countries have low uptake of existing methods of heavy metal removal from waste waters such as ion exchange, reverse osmosis, and electrodialysis due to high costs of installation, operation, and maintenance.

(2) Low-cost zeolites are efficient heavy metal adsorbents and allow modification to simultaneously remove both organic and inorganic water contaminants.

(3) Utilization of agro-wastes in the synthesis of zeolites for the removal of heavy metals is biased towards rice husk ash and bagasse ash. Other kinds of agro-wastes have not been explored.

(4) Hydrothermal synthesis of zeolites remains to be the most dominant method of zeolite synthesis even though other greener methods exist.

(5) Clay minerals have seen tremendous utilization in the synthesis of zeolites due to high silica to alumina ratios. Kaolin is especially a favorite among researchers, due to the formation of metakaolin, which is highly reactive and rich in aluminosilicates.

9. Areas of Future Research

Based on the reviewed works herein, the authors recommend following potential areas of future research:

(1) Cost-benefit analysis of clay and agro-waste zeolite application in heavy metal removal from waste waters

(2) Mechanism of removal of heavy metals and other contaminants by zeolites from contaminated water

(3) Incorporation of zeolites into other structures to form composite materials for water decontamination

(4) Impact of interfering elements on the removal of heavy metals by zeolites

(5) Criteria for eligibility of an agro-waste material as a raw material for zeolite synthesis

(6) Influence of synthesis methods on the cost, structure, application, and reproducibility of zeolites

(7) Influence of raw material source, type, and environment on the structure of synthesized zeolite

(8) Acceptability, adoption, and utilization of green chemistry methods of synthesis of zeolites, in developing countries

(9) Optimization of thermodynamic models for the analysis of all processes in zeolite heavy metal adsorption

Data Availability

Data cited are included in the cited articles.

Conflicts of Interest

The authors declare no conflicts of interest in the publication of this article.

Acknowledgments

References

[1] J. A. Nathanson, "Watewater treatment," 2021, https://www.britannica.com/technology/wastewater-treatment.

[2] WWDR. UN, "Wastewater, the untapped resource," 2017, http://www.unesco.org/new/en/natural-sciences/environment/water/wwap/wwdr/2017-wastewater-the-untapped-resource/.

[3] WHO, "People globally do not have access to safe drinking water—UNICEF," 2021, https://www.who.int/news/item/18-06-2019-1-in-3-people-globally-do-not-have-access-to-safe-drinking-water-unicef-who.

[4] K. Maheshwari, M. Agrawal, and A. B. Gupta, *Dye Pollution in Water and Wastewater*, Springer, Berlin, Germany, 2021.

[5] S. M. Wabaidur, M. A. Khan, M. R. Siddiqui et al., "Oxygenated functionalities enriched MWCNTs decorated with silica coated spinel ferrite – a nanocomposite for potentially rapid and efficient de-colorization of aquatic environment," *Journal of Molecular Liquids*, vol. 317, p. 113916, 2020.

[6] E. R. Kenawy, A. A. Ghfar, S. M. Wabaidur et al., "Cetyltrimethylammonium bromide intercalated and branched polyhydroxystyrene functionalized montmorillonite clay to sequester cationic dyes," *Journal of Environmental Management*, vol. 219, pp. 285–293, 2018.

[7] UNEP, "A snapshot of the world' s water quality: towards a global assessment," 2016, https://uneplive.unep.org/media/docs/assessments/unep_wwqa_report_web.pdf.

[8] A. Székács, "Herbicide mode of action," *In R. Mesnage & J. G. Zaller (Eds.), Herbicides*, Elsevier, Amsterdam, Netherlands, pp. 41–86, 2021.

[9] I. Ali, O. M. L. Alharbi, Z. A. ALOthman, A. M. Al-Mohaimeed, and A. Alwarthan, "Modeling of fenuron pesticide adsorption on CNTs for mechanistic insight and removal in water," *Environmental Research*, vol. 170, pp. 389–397, 2019.

[10] R. Sharma, P. R. Agrawal, R. Kumar, G. Gupta, and Ittishree, "Current scenario of heavy metal contamination in water," *In A. Ahamad, S. I. Siddiqui, & P. Singh (Eds.) Contamination of Water*, 1st edn, Elsevier, Amsterdam, Netherlands, pp. 49–64, 2021.

[11] D. Mara, "What is domestic wastewater and why treat it?" in *Domestic Wastewater Treatment in Developing Countries*, pp. 18–24, Routledge, London, UK, 2013.

[12] T. S. Anirudhan and P. S. Suchithra, "Heavy metals uptake from aqueous solutions and industrial wastewaters by humic acid-immobilized polymer/bentonite composite: kinetics and equilibrium modeling," *Chemical Engineering Journal*, vol. 156, no. 1, pp. 146–156, 2010.

[13] J. D. Edwards, "Characterizing your wastewater," *Industrial Wastewater Treatment*, 1st edn, CRC Press, Boca Raton, FL, USA, pp. 9–31, 2020.

[14] T. M. Mungai and J. Wang, "Heavy metal pollution in suburban topsoil of nyeri, kapsabet, voi, ngong and juja towns, in Kenya," *SN Applied Sciences*, vol. 9, no. 9, pp. 960–1011, 2019.

[15] C. Ohm, "Treating water pollution. water pollution," 2018, https://www.water-pollution.org.uk/treating-water-pollution/.

[16] G. K. Kinuthia, V. Ngure, D. Beti, R. Lugalia, A. Wangila, and L. Kamau, "Levels of heavy metals in wastewater and soil samples from open drainage channels in Nairobi, Kenya: community health implication," *Scientific Reports*, vol. 10, no. 1, pp. 8434–8513, 2020.

[17] M. Jamshidian, B. Sadeghalvad, I. Ghasemi, H. Ebrahimi, and I. Rezaeian, "Fabrication of polyethersulfone/functionalized MWCNTs nanocomposite and investigation its efficiency as an adsorbent of Pb (II) ions," *Arabian Journal for Science and Engineering*, vol. 46, no. 7, pp. 6259–6273, 2020.

[18] A. Mittal, M. Naushad, G. Sharma, Z. A. Alothman, S. M. Wabaidur, and M. Alam, "Fabrication of MWCNTs/ThO2 nanocomposite and its adsorption behavior for the removal of Pb (II) metal from aqueous medium," *Desalination and Water Treatment*, vol. 57, no. 46, pp. 21863–21869, 2015.

[19] A. A. Alqadami, M. Naushad, Z. A. ALOthman, M. Alsuhybani, and M. Algamdi, "Excellent adsorptive performance of a new nanocomposite for removal of toxic Pb (II) from aqueous environment: adsorption mechanism and modeling analysis," *Journal of Hazardous Materials*, vol. 389, Article ID 121896, 2020.

[20] R. Guillossou, J. le Roux, R. Mailler et al., "Organic micropollutants in a large wastewater treatment plant: what are the benefits of an advanced treatment by activated carbon adsorption in comparison to conventional treatment?" *Chemosphere*, vol. 218, pp. 1050–1060, 2019.

[21] J. Carmody, "Water treatment in developing countries | office of sustainability - student blog," 2020, https://usfblogs.usfca.edu/sustainability/2020/04/17/water-treatment-in-developing-countries/.

[22] LennTech, "Heavy metals," 2017, https://www.lenntech.com/processes/heavy/heavy-metals/heavy-metals.htm.

[23] G. van de Walle, "Iron deficiency anemia symptoms," 2022, https://www.healthline.com/nutrition/iron-deficiency-signs-symptoms.

[24] S. Y. Morris and E. Klein, "Copper and nutrition: why It's good for you. nutrition," 2021, https://www.healthline.com/health/heavy-metal-good-for-you-copper.

[25] J. Kubala, "Zinc: benefits, deficiency, food sources and side effects. nutrition," 2018, https://www.healthline.com/nutrition/zinc.

[26] M. Jaishankar, T. Tseten, N. Anbalagan, B. B. Mathew, and K. N. Beeregowda, "Toxicity, mechanism and health effects of some heavy metals," *Interdisciplinary Toxicology*, vol. 7, no. 2, pp. 60–72, 2014.

[27] A. Puri and M. Kumar, "A review of permissible limits of drinking water," *Indian Journal of Occupational and Environmental Medicine*, vol. 16, no. 1, pp. 40–44, 2012.

[28] Z. Fu and S. Xi, "The effects of heavy metals on human metabolism," *Toxicology Mechanisms and Methods*, vol. 30, no. 3, pp. 167–176, 2020.

[29] G. Georgiou, "Effects of heavy metals on human health. health effects of heavy metals," 2022, https://www.detoxmetals.com/effects-of-heavy-metals-on-human-health/?v=518f4a738816.

[30] E. I. Ugwu, A. Othmani, and C. C. Nnaji, "A review on zeolites as cost-effective adsorbents for removal of heavy metals from aqueous environment," *International journal of Environmental Science and Technology*, vol. 19, no. 8, pp. 8061–8084, 2021.

[31] N. R. Jyothi, "Heavy metal sources and their effects on human health," 2020, https://www.intechopen.com/chapters/74650.

[32] K. G. Bhattacharyya and S. S. Gupta, "Adsorptive accumulation of Cd (II), Co (II), Cu (II), Pb (II) and Ni (II) ions from water onto Kaolinite: influence of acid activation," *Adsorption Science and Technology*, vol. 27, no. 1, pp. 47–68, 2009.

[33] C. Warwick, A. Guerreiro, and A. Soares, "Sensing and analysis of soluble phosphates in environmental samples: a review," *Biosensors and Bioelectronics*, vol. 41, no. 1, pp. 1–11, 2013.

[34] M. Naushad, G. Sharma, and Z. A. Alothman, "Photodegradation of toxic dye using Gum Arabic-crosslinked-poly (acrylamide)/Ni (OH)2/FeOOH nanocomposites hydrogel," *Journal of Cleaner Production*, vol. 241, Article ID 118263, 2019.

[35] G. Crini and E. Lichtfouse, "Advantages and disadvantages of techniques used for wastewater treatment," *Environmental Chemistry Letters*, vol. 17, no. 1, pp. 145–155, 2019.

[36] R. M. Abdullah, H. Ali, and M. Mohammed, "Characteristics of erbil wastewater," 2020, https://www.researchgate.net/profile/Hiwa-Ali-2/publication/342004577_characteristics_of_erbil_wastewater/links/5ede1c8892851cf13868fc48/characteristics-of-erbil-wastewater.pdf.

[37] V. Gautam, "Preliminary treatment of sewage: 4 appurtenances. waste management," 2016, https://www.engineeringenotes.com/waste-management/sewage/preliminary-treatment-of-sewage-4-appurtenances-waste-management/39922.

[38] D. Alving, R. Arnold, J. Hunsicker et al., "Sustainable greywater filtration on a residential scale," 2019, https://drum.lib.umd.edu/handle/1903/24766.

[39] H. Bridle, K. Jacobsson, and A. C. Schultz, "Sample Processing," *Waterborne Pathogens: Detection Methods and Applications*, pp. 67–114, 2013.

[40] A. Sonune and R. Ghate, "Developments in wastewater treatment methods," *Desalination*, vol. 167, pp. 55–63, 2004.

[41] M. Sautya, "Primary treatment process of sewage. civil engineering," 2018, https://civilnoteppt.com/primary-treatment-process-of-sewage/.

[42] J. P. Guyer, "Introduction to primary wastewater treatment," *CED Engineering*, vol. 12, 2011.

[43] R. E. Hall, "Secondary wastewater treatment apparatus. appropedia," 2009, https://www.appropedia.org/Secondary_wastewater_treatment.

[44] M. L. Davis and S. J. Masten, *Principles of Environmental Engineering and Science*, McGraw-Hill Companies, New York, NY, USA, 2004.

[45] E. Massi, "Anaerobic digestion," *Fuel Cells in the Waste-to-Energy Chain*, vol. 45, pp. 47–63, 2012.

[46] M. L. Sikosana, K. Sikhwivhilu, R. Moutloali, and D. M. Madyira, "Municipal wastewater treatment technologies: a review," *Procedia Manufacturing*, vol. 35, pp. 1018–1024, 2019.

[47] T. Frankel, "What is tertiary wastewater treatment, and how does it work? smart ideas for water," 2020, https://www.ssiaeration.com/what-is-tertiary-wastewater-treatment/.

[48] T. A. McDonald and H. Komulainen, "Carcinogenicity of the chlorination disinfection by-product MX," *Journal of Environmental Science and Health, Part C*, vol. 23, no. 2, pp. 163–214, 2005.

[49] CDC, "Disinfection by-products," 2016, https://www.cdc.gov/healthywater/global/household-water-treatment/chlorination-byproducts.html?CDC_AA_refVal=https%3A%2F%2Fwww.cdc.gov%2Fsafewater%2Fchlorination-byproducts.html.

[50] K. Ikehata and Y. Li, "Ozone-based processes," *Advanced Oxidation Processes for Waste Water Treatment*, pp. 115–134, 2018.

[51] J. Väänänen, *Microsieving in Municipal Wastewater Treatment: Chemically Enhanced Primary and Tertiary Treatment*, Department of Chemical Engineering, Lund University, Lund, Sweden, 2017.

[52] B. M. Wilén, M. Cimbritz, T. Pettersson, and A. Mattsson, "Large scale tertiary filtration – results and experiences from the discfilter plant at the Rya WWTP in Sweden," *Water Practice and Technology*, vol. 11, no. 3, pp. 547–555, 2016.

[53] R. Chakraborty, A. Asthana, A. K. Singh, B. Jain, and A. B. H. Susan, "Adsorption of heavy metal ions by various low-cost adsorbents: a review," *International Journal of Environmental Analytical Chemistry*, vol. 102, no. 2, pp. 342–379, 2022.

[54] C. Cobzaru and V. Inglezakis, "Ion exchange," *Progress in Filtration and Separation*, pp. 425–498, Academic Press, Cambridge, MA, USA, 2015.

[55] P. de Luca, I. Bernaudo, R. Elliani, A. Tagarelli, J. BNagy, and A. Macario, "Industrial waste treatment by ETS-10 ion exchanger material," *Materials*, vol. 11, p. 2316, 2018.

[56] V. Kumar and V Kumar, "Adsorption kinetics and isotherms for the removal of rhodamine B dye and Pb+ 2 ions from aqueous solutions by a hybrid ion-exchanger," *Arabian Journal of Chemistry*, vol. 12, no. 3, pp. 316–329, 2019.

[57] A. Ma, A. Abushaikha, S. J. Allen, and G. McKay, "Ion exchange homogeneous surface diffusion modelling by binary site resin for the removal of nickel ions from wastewater in fixed beds," *Chemical Engineering Journal*, vol. 358, pp. 1–10, 2019.

[58] H. Esmaeili and R. Foroutan, "Investigation into ion exchange and adsorption methods for removing heavy metals from aqueous solutions," *International Journal of Biology, Pharmacy and Allied Sciences*, vol. 4, no. 12, pp. 626–629, 2015.

[59] N. K. Soliman and A. F. Moustafa, "Industrial solid waste for heavy metals adsorption features and challenges; a review," *Journal of Materials Research and Technology*, vol. 9, no. 5, pp. 10235–10253, 2020.

[60] Z. F. Pan and L. An, "Removal of heavy metal from wastewater using ion exchange membranes," in *Applications of Ion Exchange Materials in the Environment*, 1st edn, Springer, Cham, Switzerlaand, pp. 25–46, 2019.

[61] C. F. Carolin, P. S. Kumar, A. Saravanan, G. J. Joshiba, and M. Naushad, "Efficient techniques for the removal of toxic heavy metals from aquatic environment: a review," *Journal of Environmental Chemical Engineering*, vol. 5, no. 3, pp. 2782–2799, 2017.

[62] D. Bonta, "Factors that impact reverse osmosis filter performance," 2019, https://www.wqpmag.com/factors-impact-reverse-osmosis-filter-performance.

[63] M. Sarai Atab, A. J. Smallbone, and A. P. Roskilly, "An operational and economic study of a reverse osmosis desalination system for potable water and land irrigation," *Desalination*, vol. 397, pp. 174–184, 2016.

[64] J. Hanford, "Zero Waste: A Look at the Future of Reverse Osmosis. Water Quality Products," 2003, https://www.wqpmag.com/zero-waste-look-future-reverse-osmosis.

[65] B. S. Thaçi and S. T. Gashi, "Reverse osmosis removal of heavy metals from wastewater effluents using biowaste materials pretreatment," *Polish Journal of Environmental Studies*, vol. 28, no. 1, pp. 337–341, 2018.

[66] A. Karunakaran, A. Chaturvedi, J. Ali, R. Singh, S. Agarwal, and M. C. Garg, "Response surface methodology-based modeling and optimization of chromium removal using spiral-wound reverse-osmosis membrane setup," *International journal of Environmental Science and Technology*, vol. 19, no. 7, pp. 5999–6010, 2021.

[67] A. R. Kavaiya and H. D. Raval, "Highly selective and antifouling reverse osmosis membrane by crosslinkers induced surface modification," *Environmental Technology*, vol. 43, 2021.

[68] A. A. Alsarayreh, M. A. Al-Obaidi, R. Patel, and I. M. Mujtaba, "Scope and limitations of modelling, simulation, and optimisation of a spiral wound reverse osmosis process-basedwater desalination," *Processes*, vol. 8, no. 5, p. 573, 2020.

[69] I. Shahonya, F. Nangolo, M. Erinosho, and E. Angula, "Scaling and fouling of reverse osmosis (RO) membrane: technical review," *Advances in Material Science and Engineering Lecture Notes in Mechanical Engineering*, Springer, Berlin, Germany, 2021.

[70] Vedantu, "Reverse Osmosis—Principle, Advantages, Disadvantages and Applications," 2018, https://www.vedantu.com/chemistry/reverse-osmosis.

[71] H. Liu, S. Peng, L. Shu, T. Chen, T. Bao, and R. L. Frost, "Magnetic zeolite NaA: synthesis, characterization based on metakaolin and its application for the removal of Cu2+, Pb2+," *Chemosphere*, vol. 91, no. 11, pp. 1539–1546, 2013.

[72] S. U. D. Khan, S. U. D. Khan, S. N. Danish, J. Orfi, U. A. Rana, and S. Haider, "Nuclear energy powered seawater desalination," *Renewable Energy Powered Desalination Handbook*, pp. 225–264, Butterworth-Heinemann, Oxford, UK, 2018.

[73] R. Singh, "Desalination and on-site energy for groundwater treatment in developing countries using fuel cells," *Emerging Membrane Technology for Sustainable Water Treatment*, pp. 135–162, Elsevier, Amsterdam, Netherlands, 2016.

[74] L. Karimi and A. Ghassemi, "How operational parameters and membrane characteristics affect the performance of electrodialysis reversal desalination systems: the state of the art," *Journal of Membrane Science and Research*, vol. 2, no. 3, pp. 111–117, 2016.

[75] D. Zarzo, "Beneficial uses and valorization of reverse osmosis brines," *Emerging Technologies for Sustainable Desalination*

Handbook, pp. 365–397, Butterworth-Heinemann, Oxford, UK, 2018.

[76] B. V. Salas, "Desalination: trends and technologies," in *Desalination, Trends and Technologies*, M. Schorr, Ed., Taylor & Francis, Oxford, UK, 9th edition, 2012.

[77] S.-C. Chua, M. H. Isa, and Y.-C. Ho, "Electrodialysis (ED) A review on the fundamental concept, advantages, limitations and future trend," *Platform: Journal of Science and Technology*, vol. 3, no. 2, pp. 14–22, 2020.

[78] M. A. Al-Ghouti and D. A. Da'ana, "Guidelines for the use and interpretation of adsorption isotherm models: a review," *Journal of Hazardous Materials*, vol. 393, Article ID 122383, 2020.

[79] A. A. Alqadami, M. A. Khan, M. R. Siddiqui, and Z. A. Alothman, "Development of citric anhydride anchored mesoporous MOF through post synthesis modification to sequester potentially toxic lead (II) from water," *Microporous and Mesoporous Materials*, vol. 261, pp. 198–206, 2018.

[80] M. J. Thyfault, "Removal of iron, zinc, and copper from waters impacted by acid mine drainage using natural zeolite," *Open Access Theses & Dissertations*, University of Texas, Austin, TX, USA, 2016.

[81] P. Pourhakkak, M. Taghizadeh, A. Taghizadeh, and M. Ghaedi, "Adsorbent," *Interface Science and Technology*, vol. 33, pp. 71–210, 2021.

[82] A. Gupta, V. Sharma, K. Sharma et al., "A review of adsorbents for heavy metal decontamination: growing approach to wastewater treatment," *Materials*, vol. 14, no. 16, p. 4702, 2021.

[83] Benoni, "What are the main types of adsorbents? adsorbent knowledge," 2018, https://www.benonitechs.com/post/what-are-the-main-types-of-adsorbents-how-about-their-typical-applications.

[84] G. Crini, E. Lichtfouse, L. D. Wilson, and N. Morin-Crini, "Conventional and non-conventional adsorbents for wastewater treatment," *Environmental Chemistry Letters*, vol. 17, no. 1, pp. 195–213, 2019.

[85] S. Dubey, D. Gusain, Y. Chandra Sharma, and F. Bux, "Adsorbents," *Batch Adsorption Process of Metals and Anions for Remediation of Contaminated Water*, CRC Press, Boca Raton, FL, USA, 2021.

[86] S. Azarfar, F. Noorbakhsh, M. Salmani, S. Ansari, R. Soleymani, and S. Sadighi, "Experimental study and characterization of activated alumina adsorbent," in *Proceedings of the Iran International Aluminum Conference (IIAC2016)*, pp. 2–7, Tehran, Iran, May, 2016.

[87] R. Prins, "On the structure of γ-Al2O3," *Journal of Catalysis*, vol. 392, pp. 336–346, 2020.

[88] T. A. Hamza, A. H. Sherif, and E. A. Abdalla, "A novel approach to reinforce provisional material using silica gel powder," *Stomatological Disease and Science*, vol. 1, no. 1, 2017.

[89] A. Larasati, G. D. Fowler, and N. J. D. Graham, "Chemical regeneration of granular activated carbon: preliminary evaluation of alternative regenerant solutions," *Environmental Sciences: Water Research & Technology*, vol. 6, no. 8, pp. 2043–2056, 2020.

[90] G. Sethia and A. Sayari, "Activated carbon with optimum pore size distribution for hydrogen storage," *Carbon*, vol. 99, pp. 289–294, 2016.

[91] P. Baile, E. Fernández, L. Vidal, and A. Canals, "Zeolites and zeolite-based materials in extraction and microextraction techniques," *Analyst*, vol. 144, no. 2, pp. 366–387, 2019.

[92] K. He, Y. Chen, Z. Tang, and Y. Hu, "Removal of heavy metal ions from aqueous solution by zeolite synthesized from fly ash," *Environmental Science and Pollution Research*, vol. 23, no. 3, pp. 2778–2788, 2015.

[93] M. Hong, L. Yu, Y. Wang et al., "Heavy metal adsorption with zeolites: the role of hierarchical pore architecture," *Chemical Engineering Journal*, vol. 359, pp. 363–372, 2019.

[94] P. J. Reeve and H. J. Fallowfield, "Natural and surfactant modified zeolites: a review of their applications for water remediation with a focus on surfactant desorption and toxicity towards microorganisms," *Journal of Environmental Management*, vol. 205, pp. 253–261, 2018.

[95] Z. Yuna, "Review of the natural, modified, and synthetic zeolites for heavy metals removal from wastewater," *Environmental Engineering Science*, vol. 33, no. 7, pp. 443–454, 2016.

[96] D. Gusain, F. Bux, and (Faizel), *Batch Adsorption Process of Metals and Anions for Remediation of Contaminated Water*, vol. 1, 1st edition, 2021.

[97] S. M. Yakout, "Effect of porosity and surface chemistry on the adsorption-desorption of uranium (VI) from aqueous solution and groundwater," *Journal of Radioanalytical and Nuclear Chemistry*, vol. 308, no. 2, pp. 555–565, 2016.

[98] C. Tang, Y. Shu, R. Zhang et al., "Comparison of the removal and adsorption mechanisms of cadmium and lead from aqueous solution by activated carbons prepared from Typha angustifolia and Salix matsudana," *RSC Advances*, vol. 7, no. 26, pp. 16092–16103, 2017.

[99] K. F. S. Richard, A. E. B. Torres, D. A. S. Maia et al., "Assessing mass transfer rates in porous adsorbents using gas adsorption microcalorimetry," *Chemical Engineering Science*, vol. 229, Article ID 115983, 2021.

[100] D. Ouyang, Y. Zhuo, L. Hu, Q. Zeng, Y. Hu, and Z. He, "Research on the adsorption behavior of heavy metal ions by porous material prepared with silicate tailings," *Minerals*, vol. 9, no. 5, p. 291, 2019.

[101] H. S. Ibrahim, T. S. Jamil, and E. Z. Hegazy, "Application of zeolite prepared from Egyptian kaolin for the removal of heavy metals: II. Isotherm models," *Journal of Hazardous Materials*, vol. 182, no. 1–3, pp. 842–847, 2010.

[102] M. F. Shehata, S. El-Shafey, N. S. Ammar, and A. M. El-Shamy, "Reduction of Cu+2 and Ni+2 ions from wastewater using mesoporous adsorbent: Effect of treated wastewater on corrosion behavior of steel pipelines," *Egyptian Journal of Chemistry*, vol. 62, no. 9, pp. 1587–1602, 2019.

[103] G. Li, C. Foo, X. Yi et al., "Induced active sites by adsorbate in zeotype materials," *Journal of the American Chemical Society*, vol. 143, no. 23, pp. 8761–8771, 2021.

[104] H. N. Tran, P. van Viet, and H. P. Chao, "Surfactant modified zeolite as amphiphilic and dual-electronic adsorbent for removal of cationic and oxyanionic metal ions and organic compounds," *Ecotoxicology and Environmental Safety*, vol. 147, pp. 55–63, 2018.

[105] Q. Qiu, X. Jiang, G. Lv et al., "Adsorption of heavy metal ions using zeolite materials of municipal solid waste incineration fly ash modified by microwave-assisted hydrothermal treatment," *Powder Technology*, vol. 335, pp. 156–163, 2018.

[106] M. Kragović, M. Stojmenović, J. Petrović et al., "Influence of alginate encapsulation on point of zero charge (pHpzc) and thermodynamic properties of the natural and Fe (III) - modified zeolite," *Procedia Manufacturing*, vol. 32, pp. 286–293, 2019.

[107] M. Qiu and C. He, "Efficient removal of heavy metal ions by forward osmosis membrane with a polydopamine modified

zeolitic imidazolate framework incorporated selective layer," *Journal of Hazardous Materials*, vol. 367, pp. 339–347, 2019.

[108] K. O. Sulaiman, M. Sajid, and K. Alhooshani, "Application of porous membrane bag enclosed alkaline treated Y-Zeolite for removal of heavy metal ions from water," *Microchemical Journal*, vol. 152, Article ID 104289, 2020.

[109] A. A. M. Daifullah, B. S. Girgis, and H. M. H. Gad, "A study of the factors affecting the removal of humic acid by activated carbon prepared from biomass material," *Colloids and Surfaces A: Physicochemical and Engineering Aspects*, vol. 235, no. 1–3, pp. 1–10, 2004.

[110] A. C. Lua, "A detailed study of pyrolysis conditions on the production of steam-activated carbon derived from oil-palm shell and its application in phenol adsorption," *Biomass Conversion and Biorefinery*, vol. 10, no. 2, pp. 523–533, 2019.

[111] B. R. Müller, "Effect of particle size and surface area on the adsorption of albumin-bonded bilirubin on activated carbon," *Carbon*, vol. 48, no. 12, pp. 3607–3615, 2010.

[112] R. Soni, S. Bhardwaj, and D. P. Shukla, "Various water-treatment technologies for inorganic contaminants: current status and future aspects," *In P. Devi, P. Singh, & S. K. Kansal (Eds.) Inorganic Pollutants in Water*, 1st edn, Elsevier, Amsterdam, Netherlands, pp. 273–295, 2020.

[113] A. Chavoshani, M. Hashemi, M. M. Amin, and S. C. Ameta, "Introduction," *Micropollutants and Challenges: Emerging in the Aquatic Environments and Treatment Processes*, Elsevier, Amsterdam, Netherlands, 2020.

[114] V. Nejadshafiee and M. R. Islami, "Adsorption capacity of heavy metal ions using sultone-modified magnetic activated carbon as a bio-adsorbent," *Materials Science and Engineering: C*, vol. 101, pp. 42–52, 2019.

[115] G. Z. Kyzas, G. Bomis, R. I. Kosheleva et al., "Nanobubbles effect on heavy metal ions adsorption by activated carbon," *Chemical Engineering Journal*, vol. 356, pp. 91–97, 2019.

[116] M. Abbasi, "Synthesis and characterization of magnetic nanocomposite of chitosan/SiO2/carbon nanotubes and its application for dyes removal," *Journal of Cleaner Production*, vol. 145, pp. 105–113, 2017.

[117] J. Xu, Z. Cao, Y. Zhang et al., "A review of functionalized carbon nanotubes and graphene for heavy metal adsorption from water: preparation, application, and mechanism," *Chemosphere*, vol. 195, pp. 351–364, 2018.

[118] S. S. Fiyadh, M. A. AlSaadi, W. Z. Jaafar et al., "Review on heavy metal adsorption processes by carbon nanotubes," *Journal of Cleaner Production*, vol. 230, pp. 783–793, 2019.

[119] C. Rodríguez and E. Leiva, "Enhanced heavy metal removal from acid mine drainage wastewater using double-oxidized multiwalled carbon nanotubes," *Molecules 2020*, vol. 25, no. 1, p. 111, 2019.

[120] T. C. Egbosiuba and A. S. Abdulkareem, "Highly efficient as-synthesized and oxidized multi-walled carbon nanotubes for copper (II) and zinc (II) ion adsorption in a batch and fixed-bed process," *Journal of Materials Research and Technology*, vol. 15, pp. 2848–2872, 2021.

[121] M. Solic, S. Maletic, M. K. Isakovski et al., "Removing low levels of Cd (II) and Pb (II) by adsorption on two types of oxidized multiwalled carbon nanotubes," *Journal of Environmental Chemical Engineering*, vol. 9, no. 4, Article ID 105402, 2021.

[122] M. Šolic, S. Maletic, M. Kragulj Isakovski et al., "Comparing the adsorption performance of multiwalled carbon nanotubes oxidized by varying degrees for removal of low levels of copper, nickel and chromium (VI) from aqueous solutions," *Water (Switzerland)*, vol. 12, no. 3, pp. 723–818, 2020.

[123] W. Zhan, L. Gao, X. Fu, S. H. Siyal, G. Sui, and X. Yang, "Green synthesis of amino-functionalized carbon nanotube-graphene hybrid aerogels for high performance heavy metal ions removal," *Applied Surface Science*, vol. 467, pp. 1122–1133, 2019.

[124] S. Deng, X. Liu, J. Liao, H. Lin, and F. Liu, "PEI modified multiwalled carbon nanotube as a novel additive in PAN nanofiber membrane for enhanced removal of heavy metal ions," *Chemical Engineering Journal*, vol. 375, 2019.

[125] I. K. Kinoti, E. M. Karanja, E. W. Nthiga, C. M. M'thiruaine, and J. M. Marangu, "Review of clay-based nanocomposites as adsorbents for the removal of heavy metals," *Journal of Chemistry*, vol. 2022, Article ID 7504626, 25 pages, 2022.

[126] W. S. Wise, "Minerals zeolites," in *Reference Module in Earth Systems and Environmental Sciences*Elsevier, Amsterdam, Netherlands, 2013.

[127] S. Golbad, "Synthesis and characterization of microporous and mesoporous zeolites from flyash for heavy metal removal from wastewater," University of Wisconsin-Milwaukee, Milwaukee, WI, USA, Master of Science, 2016.

[128] F. R. Ribeiro, "Zeolites: science and technology," *Springer Science & Business Media*, vol. 80, 2012.

[129] S. Mitchell, A. B. Pinar, J. Kenvin, P. Crivelli, J. Kärger, and J. Pérez-Ramírez, "Structural analysis of hierarchically organized zeolites," *Nature Communications*, vol. 6, pp. 8633–8714, 2015.

[130] N. Koshy and D. N. Singh, "Fly ash zeolites for water treatment applications," *Journal of Environmental Chemical Engineering*, vol. 4, no. 2, pp. 1460–1472, 2016.

[131] A. M. Salih, "The purification of industrial wastewater to remove heavy metals and investigation into the use of zeolite as a remediation tool," in *Doctoral Dissertation*University of Wolverhampton, Wolverhampton, UK, 2018.

[132] Y. Wang, C. Wang, L. Wang, L. Wang, and F. S. Xiao, "Zeolite fixed metal nanoparticles: new perspective in catalysis," *Accounts of Chemical Research*, vol. 54, no. 11, pp. 2579–2590, 2021.

[133] S. Tajik, H. Beitollahi, F. G. Nejad et al., "Recent electrochemical applications of metal–organic framework-based materials," *Crystal Growth & Design*, vol. 20, no. 10, pp. 7034–7064, 2020.

[134] J. Behin, E. Ghadamnan, and H. Kazemian, "Recent advances in the science and technology of natural zeolites in Iran," *Clay Minerals*, vol. 54, no. 2, pp. 131–144, 2019.

[135] K. Margeta and A. Farkaš, "Introductory chapter: zeolites - from discovery to new applications on the global market," in *Zeolites - New Challenges*, pp. 1026–1056, Intechopen, London, UK, 2020.

[136] J. D. Grice, G. Raade, and M. A. Cooper, "Alflarsenite: structure and relationship to other Be-Si and zeolite framework structures," *The Canadian Mineralogist*, vol. 48, no. 2, pp. 255–266, 2010.

[137] A. Alberti, G. Vezzalini, and IUCr, "The crystal structure of amicite, a zeolite," *Acta Crystallographica Section B Structural Crystallography and Crystal Chemistry*, vol. 35, no. 12, pp. 2866–2869, 1979.

[138] A. Yu. Likhacheva, S. v. Rashchenko, and Yu. v. Seryotkin, "The deformation mechanism of a pressure-induced phase transition in dehydrated analcime," *Mineralogical Magazine*, vol. 76, no. 1, pp. 129–142, 2012.

[139] L. N. Warr, "Ima–cnmnc approved mineral symbols," *Mineralogical Magazine*, vol. 85, no. 3, pp. 291–330, 2021.

[140] D. G. Howard, R. W. Tschernich, J. v Smith, and G. L. Klein, "Boggsite, a new high-silica zeolite from goble, columbia

county, Oregon," *American Mineralogist*, vol. 75, no. 9–10, pp. 1200–1204, 1990.

[141] M. Akizuki, Y. Kudoh, and T. Kuribayashi, "Crystal structures of the {011}, {610}, and {010} growth sectors in brewsterite," *American Mineralogist*, vol. 81, no. 11–12, pp. 1501–1506, 1996.

[142] A. Augustyn, "Silicate mineral," 2020, https://www.britannica.com/science/silicate-mineral.

[143] C. J. Rhodes, "Properties and applications of zeolites," *Science Progress*, vol. 93, no. 3, pp. 223–284, 2010.

[144] S. M. Auerbach, K. A. Carrado, and P. K. Dutta, *Handbook of Zeolite Science and Technology*, CRC Press, Boca Raton, FL, USA, 2003.

[145] H. S. Sherry, "The ion-exchange properties of zeolites. I. Univalent ion exchange in synthetic faujasite," *Journal of Physical Chemistry*, vol. 70, no. 4, pp. 1158–1168, 2002.

[146] S. H. Lee, D. K. Lee, C. H. Shin et al., "Synthesis, characterization, and catalytic properties of zeolites IM-5 and NU-88," *Journal of Catalysis*, vol. 215, no. 1, pp. 151–170, 2003.

[147] L. H. Chen, M. H. Sun, Z. Wang, W. Yang, Z. Xie, and B. L. Su, "Hierarchically structured zeolites: from design to application," *Chemical Reviews*, vol. 120, no. 20, pp. 11194–11294, 2020.

[148] E. Kianfar, "Nanozeolites: synthesized, properties, applications," *Journal of Sol-Gel Science and Technology*, vol. 91, no. 2, pp. 415–429, 2019.

[149] J. Xu, Q. Wang, and F. Deng, "Metal active sites and their catalytic functions in zeolites: insights from solid-state NMR spectroscopy," *Accounts of Chemical Research*, vol. 52, no. 8, pp. 2179–2189, 2019.

[150] E. Cherian, G. Kalavathy, T. J. Joshi, M. G. Lydia Phoebe, and B. Gurunathan, "Importance of nanocatalyst and its role in biofuel production," *Biofuels and Bioenergy*, pp. 171–182, Elsevier, Amsterdam, Netherlands, 2022.

[151] S. Prodinger and M. A. Derewinski, "Synthetic zeolites and their characterization," *Nanoporous Materials for Molecule Separation and Conversion*, pp. 65–88, Elsevier, Amsterdam, Netherlands, 2020.

[152] A. Khaleque, M. M. Alam, M. Hoque et al., "Zeolite synthesis from low-cost materials and environmental applications: a review," *Environmental Advances*, vol. 2, Article ID 100019, 2020.

[153] M. Król, "Natural vs. Synthetic zeolites," *Crystals*, vol. 10, no. 7, p. 622, 2020.

[154] E. Sarti, T. Chenet, L. Pasti, A. Cavazzini, E. Rodeghero, and A. Martucci, "Effect of silica alumina ratio and thermal treatment of beta zeolites on the adsorption of toluene from aqueous solutions," *Minerals*, vol. 7, no. 2, p. 22, 2017.

[155] S. Shandong, "Factors affecting the synthesis of zeolite molecular sieves," 2021, https://www.sunhighrising.com/info/factors-affecting-the-synthesis-of-zeolite-60384086.html.

[156] H. S. Min, N. Ahmad Nizam, A. Osumanu Haruna Professor, and P. Adeniyi Alaba, *Zeolites: Synthesis, Characterisation & Practice*, P. Nagar, Ed., Ideal International E-Publication, Indore, India, 2017.

[157] I. Petrov and T. Michalev, "Synthesis of zeolite A: a review," *Proceedings—Chemical Technologies*, vol. 51, 2012.

[158] A. Feng, Y. Yu, L. Mi, Y. Cao, Y. Yu, and L. Song, "Synthesis and characterization of hierarchical Y zeolites using NH4HF2 as dealumination agent," *Microporous and Mesoporous Materials*, vol. 280, pp. 211–218, 2019.

[159] D. Georgiev, B. Bogdanov, K. Angelova, I. Markovska, and Y. Hristov, "Synthetic zeolites- structure, classification,

[160] Z. Zijun, G. Effeney, G. J. Millar, and M. Stephen, "Synthesis and cation exchange capacity of zeolite W from ultra-fine natural zeolite waste," *Environmental Technology & Innovation*, vol. 23, Article ID 101595, 2021.

[161] D. Georgiev, B. Bogdanov, I. Markovska, and Y. Hristov, "A study on the synthesis and structure of zeolite NaX," *Journal of Chemical Technology and Metallurgy*, vol. 48, no. 2, pp. 168–173, 2013.

[162] Y. Zhao, Z. Liu, W. Li et al., "Synthesis, characterization, and catalytic performance of high-silica Y zeolites with different crystallite size," *Microporous and Mesoporous Materials*, vol. 167, pp. 102–108, 2013.

[163] D. Georgiev, B. Bogdanov, Y. Hristov, and I. Markovska, "Synthesis of NaA zeolite from natural kaolinite," *Oxidation Communications*, vol. 34, no. 4, pp. 812–819, 2011.

[164] J. Han, X. Jin, C. Song et al., "Rapid synthesis and NH3 -SCR activity of SSZ-13 zeolite via coal gangue," *Green Chemistry*, vol. 22, no. 1, pp. 219–229, 2020.

[165] S. Krachuamram, K. C. Chanapattharapol, and N. Kamonsutthipaijit, "Synthesis and characterization of NaX-type zeolites prepared by different silica and alumina sources and their CO2 adsorption properties," *Microporous and Mesoporous Materials*, vol. 310, Article ID 110632, 2021.

[166] F. García-Villén, E. Flores-Ruíz, C. Verdugo-Escamilla, and F. J. Huertas, "Hydrothermal synthesis of zeolites using sanitary ware waste as a raw material," *Applied Clay Science*, vol. 160, pp. 238–248, 2018.

[167] Y. Li, R. Zhao, Y. Pang, X. Qiu, and D. Yang, "Microwave-assisted synthesis of high carboxyl content of lignin for enhancing adsorption of lead," *Colloids and Surfaces A: Physicochemical and Engineering Aspects*, vol. 553, pp. 187–194, 2018.

[168] W. M. Xie, F. P. Zhou, X. L. Bi et al., "Accelerated crystallization of magnetic 4A-zeolite synthesized from red mud for application in removal of mixed heavy metal ions," *Journal of Hazardous Materials*, vol. 358, pp. 441–449, 2018.

[169] Z. Tauanov, D. Shah, V. Inglezakis, and P. K. Jamwal, "Hydrothermal synthesis of zeolite production from coal fly ash: a heuristic approach and its optimization for system identification of conversion," *Journal of Cleaner Production*, vol. 182, pp. 616–623, 2018a.

[170] Y. Kobayashi, F. Ogata, T. Nakamura, and N. Kawasaki, "Synthesis of novel zeolites produced from fly ash by hydrothermal treatment in alkaline solution and its evaluation as an adsorbent for heavy metal removal," *Journal of Environmental Chemical Engineering*, vol. 8, no. 2, Article ID 103687, 2020.

[171] H. Luo, W. W. Law, Y. Wu, W. Zhu, and E. H. Yang, "Hydrothermal synthesis of needle-like nanocrystalline zeolites from metakaolin and their applications for efficient removal of organic pollutants and heavy metals," *Microporous and Mesoporous Materials*, vol. 272, pp. 8–15, 2018.

[172] G. Yao, J. Lei, X. Zhang, Z. Sun, and S. Zheng, "One-step hydrothermal synthesis of zeolite X powder from natural low-grade diatomite," *Materials*, vol. 11, no. 6, p. 906, 2018.

[173] J. Che, X. Yao, J. Kong et al., "Molten-salt synthesis and spectral characteristics of perovskite KCa2Nb3O10:Sm3+ phosphors," *Journal of Luminescence*, vol. 244, Article ID 118665, 2022.

[174] M. Maharana and S. Sen, *Fly-Ash Derived Zeolite as a Versatile Novel Material in Civil Engineering: An Overview*, Springer, Berlin, Germany, 2021.

[175] H. Susanto, N. A. C. Imani, N. R. Aslamiyah, T. Istirokhatun, and M. H. Robbani, "The effect of an ultrasound radiation on the synthesis of 4A zeolite from fly ash," *IOP Conference Series: Materials Science and Engineering*, vol. 367, no. 1, Article ID 012026, 2018.

[176] K. Ojha, N. C. Pradhan, and A. N. Samanta, "Zeolite from fly ash: synthesis and characterization," *Bulletin of Materials Science*, vol. 27, no. 6, pp. 555–564, 2004.

[177] M. Park, C. L. Choi, W. T. Lim, M. C. Kim, J. Choi, and N. H. Heo, "Molten-salt method for the synthesis of zeolitic materials: I. Zeolite formation in alkaline molten-salt system," *Microporous and Mesoporous Materials*, vol. 37, no. 1–2, pp. 81–89, 2000.

[178] X. Querol, N. Moreno, J. Umaña et al., "Synthesis of zeolites from coal fly ash: an overview," *International Journal of Coal Geology*, vol. 50, no. 1–4, pp. 413–423, 2002.

[179] Q. Miao, B. Zhao, S. Liu, J. Guo, Y. Tong, and J. Cao, "Decomposition of the potassic rocks by sub-molten salt method and synthesis of low silica X zeolite," *Asia-Pacific Journal of Chemical Engineering*, vol. 11, no. 4, pp. 558–566, 2016.

[180] J. Yang, T. Li, X. Bao, Y. Yue, and H. Liu, "Mesoporogen-free synthesis of hierarchical sodalite as a solid base catalyst from sub-molten salt-activated aluminosilicate," *Particuology*, vol. 48, pp. 48–54, 2020.

[181] Y. Meng, B. Zhao, H. Zhang, X. Liu, and J. Cao, "Synthesis of zeolite W from potassic rocks activated by KOH sub-molten salt method," *Crystal Research and Technology*, vol. 53, no. 6, Article ID 1700216, 2018.

[182] Y. K. Krisnandi, I. Mahmuda, D. U. C. Rahayu, and R. Sihombing, "Synthesis and characterization of ZSM-5 zeolite from dealuminated and fragmentated bayat-klaten natural zeolite," *Journal of Physics: Conference Series*, vol. 1095, no. 1, Article ID 012044, 2018.

[183] Y. H. Hsiao, T. Y. Ho, Y. H. Shen, and D. Ray, "Synthesis of analcime from sericite and pyrophyllite by microwave-assisted hydrothermal processes," *Applied Clay Science*, vol. 143, pp. 378–386, 2017.

[184] X. Zeng, X. Hu, H. Song et al., "Microwave synthesis of zeolites and their related applications," *Microporous and Mesoporous Materials*, vol. 323, Article ID 111262, 2021.

[185] A. R. Majdinasab, P. K. Manna, Y. Wroczynskyj et al., "Cost-effective zeolite synthesis from waste glass cullet using energy efficient microwave radiation," *Materials Chemistry and Physics*, vol. 221, pp. 272–287, 2019.

[186] S. F. Wong, K. Deekamwong, J. Wittakayun et al., "Nano-crystalline K-F zeolite from rice husk silica as an eco-friendly solid base catalyst for the synthesis of jasminaldehyde under microwave irradiation," *Sains Malaysiana*, vol. 47, no. 2, pp. 337–345, 2018.

[187] N. Soltani, A. Bahrami, M. I. Pech-Canul, and L. A. González, "Review on the physicochemical treatments of rice husk for production of advanced materials," *Chemical Engineering Journal*, vol. 264, pp. 899–935, 2015.

[188] S. Bohra, D. Kundu, and M. K. Naskar, "One-pot synthesis of NaA and NaP zeolite powders using agro-waste material and other low cost organic-free precursors," *Ceramics International*, vol. 40, no. 1, pp. 1229–1234, 2014.

[189] V. P. Mallapur and J. U. K. Oubagaranadin, "A brief review on the synthesis of zeolites from hazardous wastes," *Transactions of the Indian Ceramic Society*, vol. 76, no. 1, pp. 1–13, 2017.

[190] S. Bohra, K. P. Dey, D. Kundu, and M. K. Naskar, "Synthesis of zeolite T powders by direct dissolution of rice husk ash: an agro-waste material," *Journal of Materials Science*, vol. 48, no. 22, pp. 7893–7901, 2013.

[191] P. Alaba, O. B. Ayodele, W. M. Ashri, and W. Daud, "Overview of the synthesis of nanozeolite from agro-waste," 2017, https://www.researchgate.net/profile/Peter-Alaba/publication/320676597_Synthesis_of_hierarchical_mesoporous_zeolite/links/5a19a1ce0f7e9be37f9a533b/Synthesis-of-hierarchical-mesoporous-zeolite.pdf#page=30.

[192] J. A. Oliveira, F. A. Cunha, and L. A. M. Ruotolo, "Synthesis of zeolite from sugarcane bagasse fly ash and its application as a low-cost adsorbent to remove heavy metals," *Journal of Cleaner Production*, vol. 229, pp. 956–963, 2019.

[193] O. B. Kotova, I. N. Shabalin, D. A. Shushkov, and L. S. Kocheva, "Hydrothermal synthesis of zeolites from coal fly ash," *Advances in Applied Ceramics*, vol. 115, no. 3, pp. 1–6, 2015.

[194] L. Deng, Q. Xu, and H. Wu, "Synthesis of zeolite-like material by hydrothermal and fusion methods using municipal solid waste fly ash," *Procedia Environmental Sciences*, vol. 31, pp. 662–667, 2016.

[195] M. Esaifan, M. Hourani, H. Khoury, H. Rahier, and J. Wastiels, "Synthesis of hydroxysodalite zeolite by alkali-activation of basalt powder rich in calc-plagioclase," *Advanced Powder Technology*, vol. 28, no. 2, pp. 473–480, 2017.

[196] Y. W. Chiang, K. Ghyselbrecht, R. M. Santos, B. Meesschaert, and J. A. Martens, "Synthesis of zeolitic-type adsorbent material from municipal solid waste incinerator bottom ash and its application in heavy metal adsorption," *Catalysis Today*, vol. 190, no. 1, pp. 23–30, 2012.

[197] M. Gross, M. Soulard, P. Caullet, J. Patarin, and I. Saude, "Synthesis of faujasite from coal fly ashes under smooth temperature and pressure conditions: a cost saving process," *Microporous and Mesoporous Materials*, vol. 104, no. 1–3, pp. 67–76, 2007.

[198] T. Wajima, T. Shimizu, and Y. Ikegami, "Synthesis of zeolites from paper sludge ash and their ability to simultaneously remove NH4+ and PO4 3−," *Journal of Environmental Science and Health, Part A*, vol. 42, no. 3, pp. 345–350, 2007.

[199] S. C. Aboudi Mana, M. M. Hanafiah, and A. J. K. Chowdhury, "Environmental characteristics of clay and clay-based minerals," *Geology, Ecology, and Landscapes*, vol. 1, no. 3, pp. 155–161, 2017.

[200] O. O. Ltaief, S. Siffert, S. Fourmentin, and M. Benzina, "Synthesis of Faujasite type zeolite from low grade Tunisian clay for the removal of heavy metals from aqueous waste by batch process: kinetic and equilibrium study," *Comptes Rendus Chimie*, vol. 18, no. 10, pp. 1123–1133, 2015.

[201] D. F. Medina, D. M. San Martin, C. M. López et al., "Removal of Pb (II) in aqueous solutions using synthesized zeolite X from Ecuadorian clay," *Ingeniería e Investigación*, vol. 41, no. 2, Article ID e89671, 2021.

[202] M. A. Moneim and E. A. Ahmed, "Synthesis of faujasite from Egyptian clays: characterizations and removal of heavy metals," *Geomaterials*, vol. 05, no. 02, pp. 68–76, 2015.

[203] A. Gaidoumi, A. Chaouni Benabdallah, B. el Bali, and A. Kherbeche, "Synthesis and characterization of zeolite HS using natural pyrophyllite as new clay source," *Arabian Journal for Science and Engineering*, vol. 43, no. 1, pp. 191–197, 2017.

[204] E. Aghaei, M. Ebrahiminejad, R. Khoshbin et al., "Synthesis of mesoporous Y zeolite from pyrophyllite as Si and Al source used in gasoline and gasoil production from heavy oil," *Fuel and Combustion*, vol. 13, no. 1, pp. 50–66, 2020.

[205] M. Foroughi, A. Salem, and S. Salem, "Potential of fusion technique in production of mesoporous zeolite A powder from poor kaolin through modification by boehmite: effect of clay mineralogy on particle morphology," *Advanced Powder Technology*, vol. 32, no. 7, pp. 2423–2432, 2021.

[206] I. v. Joseph, L. Tosheva, G. Miller, and A. M. Doyle, "FAU-type zeolite synthesis from clays and its use for the simultaneous adsorption of five divalent metals from aqueous solutions," *Materials 2021*, vol. 14, no. 13, p. 3738, 2021.

[207] M. Omidi, A. Fatehinya, M. Farahani et al., "Characterization of biomaterials," *Biomaterials for Oral and Dental Tissue Engineering*, vol. 97–115, pp. 97–115, 2017.

[208] S. Nasrazadani and S. Hassani, "Modern analytical techniques in failure analysis of aerospace, chemical, and oil and gas industries," *Handbook of Materials Failure Analysis with Case Studies from the Oil and Gas Industry*, pp. 39–54, Butterworth-Heinemann, Oxford, UK, 2016.

[209] I. v. Joseph, L. Tosheva, and A. M. Doyle, "Simultaneous removal of Cd (II), Co (II), Cu (II), Pb (II), and Zn (II) ions from aqueous solutions via adsorption on FAU-type zeolites prepared from coal fly ash," *Journal of Environmental Chemical Engineering*, vol. 8, no. 4, Article ID 103895, 2020.

[210] Z. Tauanov, P. E. Tsakiridis, S. v. Mikhalovsky, and V. J. Inglezakis, "Synthetic coal fly ash-derived zeolites doped with silver nanoparticles for mercury (II) removal from water," *Journal of Environmental Management*, vol. 224, pp. 164–171, 2018b.

[211] M. A. Ismail, M. A. Z. Eltayeb, and S. A. A. Maged, "Synthesis of zeolite A from Sudanese montmorillonite clay to remove nickel and copper ions from aqueous solutions," *IJCBS*, vol. 4, pp. 46–56, 2013.

[212] V. Wernert, O. Schaef, L. Aloui et al., "Cancrinite synthesis from natural kaolinite by high pressure hydrothermal method: application to the removal of Cd2+ and Pb2+ from water," *Microporous and Mesoporous Materials*, vol. 301, Article ID 110209, 2020.

[213] P. Labs, "Bet specific surface area—particle techology labs," 2011, https://www.particletechlabs.com/analytical-testing/gas-adsorption-and-porosimetry/bet-specific-surface-area.

[214] M. Nasrollahzadeh, M. Atarod, M. Sajjadi, S. M. Sajadi, and Z. Issaabadi, "Plant-mediated green synthesis of nanostructures: mechanisms, characterization, and applications," *Interface Science and Technology*, vol. 28, pp. 199–322, 2019.

[215] W. Feng, Z. Wan, J. Daniels et al., "Synthesis of high quality zeolites from coal fly ash: mobility of hazardous elements and environmental applications," *Journal of Cleaner Production*, vol. 202, pp. 390–400, 2018.

[216] G. K. R. Angaru, Y. L. Choi, L. P. Lingamdinne et al., "Facile synthesis of economical feasible fly ash–based zeolite–supported nano zerovalent iron and nickel bimetallic composite for the potential removal of heavy metals from industrial effluents," *Chemosphere*, vol. 267, Article ID 128889, 2021.

[217] T. Amiri-Yazani, R. Zare-Dorabei, M. Rabbani, and A. Mollahosseini, "Highly efficient ultrasonic-assisted preconcentration and simultaneous determination of trace amounts of Pb (II) and Cd (II) ions using modified magnetic natural clinoptilolite zeolite: response surface methodology," *Microchemical Journal*, vol. 146, pp. 498–508, 2019.

[218] D. Czarna, P. Baran, P. Kunecki, R. Panek, R. Żmuda, and M. Wdowin, "Synthetic zeolites as potential sorbents of mercury from wastewater occurring during wet FGD processes of flue gas," *Journal of Cleaner Production*, vol. 172, pp. 2636–2645, 2018.

[219] P. S. Nayak and B. K. Singh, "Instrumental characterization of clay by XRF, XRD and FTIR," *Bulletin of Materials Science*, vol. 30, no. 3, pp. 235–238, 2007.

[220] R. Kohli and K. Mittal, "Methods for assessing surface cleanliness," *Developments in Surface Contamination and Cleaning*, vol. 12, pp. 23–105, 2019.

[221] N. Goyal, S. Barman, and V. K. Bulasara, "Efficient removal of bisphenol S from aqueous solution by synthesized nano-zeolite secony mobil-5," *Microporous and Mesoporous Materials*, vol. 259, pp. 184–194, 2018.

[222] M. A. Khan, A. A. Alqadami, S. M. Wabaidur et al., "Oil industry waste based non-magnetic and magnetic hydrochar to sequester potentially toxic post-transition metal ions from water," *Journal of Hazardous Materials*, vol. 400, Article ID 123247, 2020.

[223] M. Rani, Keshu, and U. Shanker, "Green nanomaterials: an overview," *Green Functionalized Nanomaterials for Environmental Applications*, pp. 43–80, Elsevier, Amsterdam, Netherlands, 2022.

[224] N. Birkner, "How an FTIR spectrometer operates," 2011, https://chem.libretexts.org/Bookshelves/Physical_and_Theoretical_Chemistry_Textbook_Maps/Supplemental_Modules_%20(Physical_and_Theoretical_Chemistry)/Spectroscopy/Vibrational_Spectroscopy/Infrared_Spectroscopy/How_an_FTIR_Spectrometer_Operates.

[225] K. Song, "Interphase characterization in rubber nanocomposites," *Progress in Rubber Nano-composites*, pp. 115–152, Elsevier, Amsterdam, Netherlands, 2017.

[226] M. Esaifan, L. N. Warr, G. Grathoff et al., "Synthesis of hydroxy-sodalite/cancrinite zeolites from calcite-bearing kaolin for the removal of heavy metal ions in aqueous media," *Minerals*, vol. 9, no. 8, p. 484, 2019.

[227] K. Ahmad, H. ur R. Shah, M. Ashfaq et al., "Effect of metal atom in zeolitic imidazolate frameworks (ZIF-8 & 67) for removal of Pb2+ & Hg2+ from water," *Food and Chemical Toxicology*, vol. 149, Article ID 112008, 2021.

[228] X. Pu, L. Yao, L. Yang, W. Jiang, and X. Jiang, "Utilization of industrial waste lithium-silicon-powder for the fabrication of novel nap zeolite for aqueous Cu (II) removal," *Journal of Cleaner Production*, vol. 265, Article ID 121822, 2020.

[229] W. Patcharin, K. Sriamporn, and A. Kanokkan, "Utilization biomass from bagasse ash for phillipsite zeolite synthesis," *Advanced Materials Research*, vol. 383–390, pp. 4038–4042, 2011.

[230] K. R. Rajisha, B. Deepa, L. A. Pothan, and S. Thomas, "Thermomechanical and spectroscopic characterization of natural fibre composites," *Interface Engineering of Natural Fibre Composites for Maximum Performance*, pp. 241–274, Woodhead Publishing, Sawston, UK, 2011.

[231] Z. Ezzeddine, I. Batonneau-Gener, Y. Pouilloux, H. Hamad, and Z. Saad, "Synthetic nax zeolite as a very efficient heavy metals sorbent in batch and dynamic conditions," *Colloids and Interfaces*, vol. 2, no. 2, p. 22, 2018.

[232] D. P. De-La-Vega, C. González, C. A. Escalante et al., "Uso de zeolita faujasita para adsorción de iones en aguas residuales municipales," *Tecnología y Ciencias Del Agua*, vol. 9, no. 4, pp. 184–208, 2018.

[233] M. R. Mirbaloochzehi, A. Rezvani, A. Samimi, and M. Shayesteh, "Application of a novel surfactant-modified natural nano-zeolite for removal of heavy metals from drinking water," *Advanced Journal of Chemistry-Section A*, vol. 2020, no. 5, pp. 612–620, 2020.

[234] D. Ao, A. P. Olalekan, and A. M. Olatunya, "Langmuir, Freundlich, Temkin and Dubinin–radushkevich Isotherms:

studies of equilibrium sorption of Zn2+ unto phosphoric acid modified rice husk," *IOSR Journal of Applied Chemistry*, vol. 3, no. 1, pp. 38–45, 2012.

[235] Z. A. Alothman, A. H. Bahkali, M. A. Khiyami et al., "Low cost biosorbents from fungi for heavy metals removal from wastewater," *Separation Science and Technology*, vol. 55, no. 10, p. 1766, Article ID 1608242, 2019.

[236] S. K. Papageorgiou, F. K. Katsaros, E. P. Kouvelos, J. W. Nolan, H. le Deit, and N. K. Kanellopoulos, "Heavy metal sorption by calcium alginate beads from Laminaria digitata," *Journal of Hazardous Materials*, vol. 137, no. 3, pp. 1765–1772, 2006.

[237] M. Tadesse, "Synthesis and characterization of zeolite a using bagasse ash, as biosilica source for water hardness removal," 2018, http://213.55.101.23/handle/123456789/949.

[238] M. Shamsayei, Y. Yamini, and H. Asiabi, "Synthesis and characterization of layered double hydroxide decorated zeolite as the efficient sorbent for removal of toxic metal ions," *Environmental Progress & Sustainable Energy*, vol. 41, no. 1, Article ID e13727, 2022.

[239] V. K. Jha, M. Nagae, M. Matsuda, and M. Miyake, "Zeolite formation from coal fly ash and heavy metal ion removal characteristics of thus-obtained Zeolite X in multi-metal systems," *Journal of Environmental Management*, vol. 90, no. 8, pp. 2507–2514, 2009.

[240] W. w. Bao, H. f. Zou, S. c. Gan, X. c. Xu, G. j. Ji, and Ky Zheng, "Adsorption of heavy metal ions from aqueous solutions by zeolite based on oil shale ash: kinetic and equilibrium studies," *Chemical Research in Chinese Universities*, vol. 29, no. 1, pp. 126–131, 2013.

[241] X. Zhang, T. Cheng, C. Chen et al., "Synthesis of a novel magnetic nano-zeolite and its application as an efficient heavy metal adsorbent," *Materials Research Express*, vol. 7, no. 8, Article ID 085007, 2020.

[242] K. S. Hui, C. Y. H. Chao, and S. C. Kot, "Removal of mixed heavy metal ions in wastewater by zeolite 4A and residual products from recycled coal fly ash," *Journal of Hazardous Materials*, vol. 127, no. 1–3, pp. 89–101, 2005.

[243] N. Ayawei, A. N. Ebelegi, and D. Wankasi, "Modelling and interpretation of adsorption isotherms," *Journal of Chemistry*, vol. 2017, Article ID 3039817, 11 pages, 2017.

[244] A. A. Inyinbor, F. A. Adekola, and G. A. Olatunji, "Kinetics, isotherms and thermodynamic modeling of liquid phase adsorption of Rhodamine B dye onto Raphia hookerie fruit epicarp," *Water Resources and Industry*, vol. 15, pp. 14–27, 2016.

[245] G. W. Kajjumba, S. Emik, A. Öngen, H. Kurtulus Özcan, and S. Aydın, "Modelling of adsorption kinetic processes—errors, theory and application," in *Advanced Sorption Process Applications* IntechOpen, London, UK, 2019.

[246] M. A. Anang, R. Zugle, and B. Sefa-Ntiri, "Assessing the adsorptive and photodegradative efficiencies of ZSM-11 synthesized from rice husk ash," *Journal of Chemistry*, vol. 2020, Article ID 6094126, 13 pages, 2020.

[247] E. A. Abdelrahman, Y. G. Abou El-Reash, H. M. Youssef, Y. H. Kotp, and R. M. Hegazey, "Utilization of rice husk and waste aluminum cans for the synthesis of some nanosized zeolite, zeolite/zeolite, and geopolymer/zeolite products for the efficient removal of Co (II), Cu (II), and Zn (II) ions from aqueous media," *Journal of Hazardous Materials*, vol. 401, Article ID 123813, 2021.

[248] T. Chuenpratoom, K. Hemavibool, K. Rermthong, and S. Nanan, "Removal of lead by merlinoite prepared from sugarcane bagasse ash and kaolin: synthesis, isotherm,

kinetic, and thermodynamic studies," *Molecules 2021*, vol. 26, p. 7550, 2021.

[249] T. Cheng, C. Chen, R. Tang, C.-H. Han, and Y. Tian, "Competitive adsorption of Cu, Ni, Pb, and Cd from aqueous solution onto fly ash-based linde F (K) zeolite," *Journal of Chemical & Engineering Data*, vol. 37, no. 1, 2018.

[250] R. M. Abdel-Hameed, E. Abdel-Aal, F. Farghaly et al., "Exploitation of industrial solid wastes for preparing zeolite as a value-added product and its kinetics as adsorbent for heavy metal ions," *Physicochemical Problems of Mineral Processing*, vol. 57, no. 1, pp. 87–99, 2020.

[251] A. Saravanan, P. S. Kumar, P. R. Yaashikaa, S. Karishma, S. Jeevanantham, and S. Swetha, "Mixed biosorbent of agro waste and bacterial biomass for the separation of Pb (II) ions from water system," *Chemosphere*, vol. 277, Article ID 130236, 2021.

[252] Z. Ghasemi, I. Sourinejad, H. Kazemian, M. Hadavifar, S. Rohani, and H. Younesi, "Kinetics and thermodynamic studies of Cr (VI) adsorption using environmental friendly multifunctional zeolites synthesized from coal fly ash under mild conditions," *Chemical Engineering Communications*, vol. 207, no. 6, pp. 808–825, 2020.

[253] S. Khandaker, Y. Toyohara, G. C. Saha, M. R. Awual, and T. Kuba, "Development of synthetic zeolites from bio-slag for cesium adsorption: kinetic, isotherm and thermodynamic studies," *Journal of Water Process Engineering*, vol. 33, Article ID 101055, 2020.

[254] J. Yang, H. Sun, T. Peng, L. Zeng, and X. Zhou, "Mild hydrothermal synthesis of 11Å-TA from alumina extracted coal fly ash and its application in water adsorption of heavy metal ions (Cu (II) and Pb (II))," *International Journal of Environmental Research and Public Health 2022*, vol. 19, 2022.

[255] L. Liu, X. B. Luo, L. Ding, and S. L. Luo, "Application of nanotechnology in the removal of heavy metal from water," *Nanomaterials for the Removal of Pollutants and Resource Reutilization*, pp. 83–147, Elsevier, Amsterdam, Netherlands, 2019.

[256] X. Liu, G. Wang, Q. Luo, X. Li, and Z. Wang, "The thermodynamics and kinetics for the removal of copper and nickel ions by the zeolite Y synthesized from fly ash," *Materials Research Express*, vol. 6, no. 2, p. 025001, 2018.